Molecular Phylogenetics and Evolution 224 (2026) 108689

Contents lists available at ScienceDirect

Molecular Phylogenetics and Evolution

journal homepage: www.elsevier.com/locate/ympev

Genome-scale molecular systematics of Madagascar's occipital-lobed chameleons reveals polyphyly and mito-nuclear discordances

Miguel Vences [a,*], Laila-Denise Rothe [a], Frank Glaw [b], Mark D. Scherz [c], Philip-Sebastian Gehring [d], Oliver Hawlitschek [e], Arianna Kuhn [f,g], Malte Multzsch [a], Alice Petzold [g], Michaela Preick [g], Fandresena Rakotoarimalala [h,i], Achille P. Raselimanana [i,j], Fanomezana M. Ratsoavina [h], Sara Ruane [j], David R. Vieites [k], Michael Hofreiter [g], Christophe Dufresnes [l]

[a] Technische Universität Braunschweig, Institute for Cell- and Neurobiology, Mendelssohnstraße 4, 38106 Braunschweig, Germany
[b] Zoologische Staatssammlung München (ZSM-SNSB), Münchhausenstraße 21, 81247 München, Germany
[c] Natural History Museum Denmark, University of Copenhagen, Universitetsparken 15, 2100 Copenhagen Ø, Denmark
[d] Jöllenbecker Heide 49d, 33739 Bielefeld, Germany
[e] Department of Evolutionary Biology and Environmental Studies, Universität Zürich, Winterthurer Str. 190, 8057 Zürich, Switzerland
[f] Illinois Natural History Survey, Prairie Research Institute, University of Illinois Urbana-Champaign, Champaign, IL 61820, USA
[g] Institute of Biochemistry and Biology, University of Potsdam, Karl-Liebknecht-Str. 24–25, 14476 Potsdam, Germany
[h] Mention Zoologie et Biodiversité Animale, Faculté des Sciences, Université d'Antananarivo, Madagascar
[i] Association Vahatra, Lot V A 38 LBA Ter Ambohidempona Tsiadana, BP 3972, Antananarivo 101 Madagascar
[j] Negaunee Integrative Research Center, Field Museum of Natural History, Chicago, IL 60605, USA
[k] Integrative Marine Ecology Group, Instituto de Investigacions Marinas (IIM-CSIC), Vigo, Spain
[l] Institut de Systématique, Evolution, Biodiversité (ISYEB), Muséum national d'Histoire naturelle, CNRS, Sorbonne Université, EPHE-PSL, Université des Antilles, 55 rue Buffon, CP 51, Paris, France

ARTICLE INFO

Keywords:
Squamata
Chamaeleonidae
Calumma brevicorne
Calumma malthe
Calumma krystalae sp.nov.
Madagascar
Species delimitation
RADseq
Museomics

ABSTRACT

Madagascar-endemic chameleons with large, conspicuous occipital lobes currently comprise 12 species that were traditionally classified in the phenetic *Calumma cucullatum* group. We here use a combination of DNA sequences from Restriction-Associated DNA sequencing (RADseq), museomics shotgun sequencing from historical name-bearing types, and Sanger-sequenced mitochondrial and nuclear gene fragments, to revisit the phylogeny and species delimitation in this group. We find robust phylogenomic evidence for polyphyly of the group, with *C. cucullatum* sister to the *C. furcifer* group, and species of the *C. nasutum* group intercalated between *C. malthe* and the remainder of ingroup species. Furthermore, according to our mitochondrial tree, *C. tsycorne* does not belong to the group. Several species such as *C. brevicorne* and *C. malthe* are recovered as paraphyletic in the mitochondrial tree while being unambiguously monophyletic in the phylogenomic tree; this mito-nuclear discordance may reflect ancestral introgressive hybridization. In our phylogenomic estimations, most currently recognized species are inferred as deep monophyletic lineages, and the RADseq clustering analysis recovered these as well-defined units. Exceptions were *C. jejy*, which is placed as sister taxon to the morphologically distinct *C. peltierorum* with rather shallow sequence divergence, and the *C. brevicorne* / *C. crypticum* complex. Combining molecular and morphological data suggests that populations of *C. malthe* from northern Madagascar represent a distinct species, here described as *C. krystalae* sp. nov. Our data reveal that chameleons, despite their elaborate phenotypic differences used in intraspecific signalling and their interspecific genital differences, can be characterized by complex evolutionary patterns probably involving hybridization and introgression.

* Corresponding author.
E-mail address: m.vences@tu-braunschweig.de (M. Vences).

https://doi.org/10.1016/j.ympev.2026.108689
Received 8 January 2026; Received in revised form 21 May 2026; Accepted 8 July 2026
Available online 10 July 2026
1055-7903/© 2026 The Author(s). Published by Elsevier Inc. This is an open access article under the CC BY license (http://creativecommons.org/licenses/by/4.0/).

1. Introduction

Chameleons are a group of lizards with numerous unique eco-morphological and behavioral adaptations (Tolley & Herrel 2013), including particular integumental structures allowing for their proverbial color change (Grbic et al. 2015; Teyssier et al. 2015). Color and color change, as well as external ornaments such as crests, casques, lobes and rostral projections, are sexually dimorphic in many chameleons, often differ between closely related species, and are known to be used in male-male combat and male–female courtship (e.g., Parcher 1974; Stuart-Fox and Moussalli, 2008; Dollion et al. 2020; Whiting et al. 2022; Keren-Rotem et al. 2024; Glaw et al. 2025). Given the characteristics and use of this ornamentation, it is likely that sexual selection has influenced the evolution of these traits (Stuart-Fox and Moussalli, 2008; Van Kleeck-Hann & Wiens 2023), and, although untested, it can be hypothesized that it also played a role in driving and reinforcing

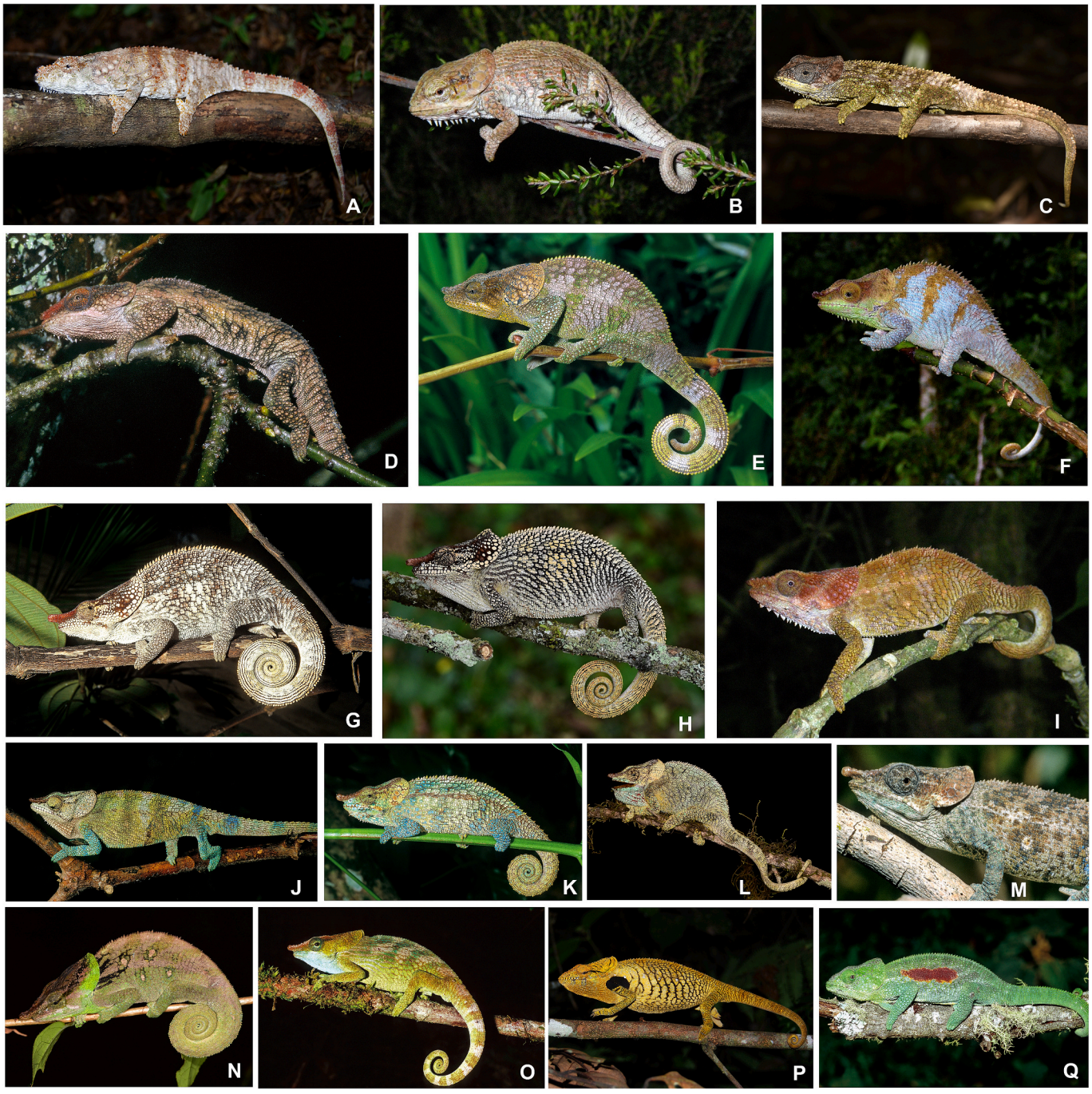

Fig. 1. Representative photos in life of male specimens of occipital-lobed chameleons assigned to the *Calumma cucullatum* group according to current classification (A) *C. hafahafa*, ZSM 511/2014, Andrevorevo; (B) *C. tsaratananense*, Tsaratanana Massif; (C) *C. jejy*, FGZC 7346, Marojejy; (D) *C. hilleniusi*, Manjakatompo; (E) *C. amber,* Montagne d'Ambre; (F) *C. peltierorum*, Tsaratanana; (G) *C. brevicorne* complex, lineage BRE5, Andasibe; (H) *C. brevicorne* complex, lineage BRE5, MVTIS 38035, Andasibe; (I) *C. brevicorne* complex, lineage BRE7, Analabe forest; (J) *C. brevicorne* complex, lineage BRE5, Mandraka; (K) *C. brevicorne* complex, lineage BRE2, Ranomafana; (L) *C. brevicorne* complex, lineage BRE2, Andringitra; (M) *C. brevicorne* complex, lineage BRE4, ZSM 546/2001, Itremo; (N), *C. malthe,* lineage MA1, Maromizaha; (O) *C. malthe* lineage MA2 (= *C. krystalae* sp. nov.), ZSM 71/2005, Marojejy; (P) *C. cucullatum* (female), Marolambo; (Q) *C. capuroni,* Andohahela. All photographs by the authors.

chameleon species boundaries (e.g., Böhme, 1988). For some species, such as the panther chameleon *Furcifer pardalis*, allopatric populations with distinct color morphs and moderate but consistently recovered mitochondrial genetic divergence have been hypothesized to represent distinct taxonomic units (Grbic et al. 2015). Other Malagasy species, such as *Calumma brevicorne*, encompass numerous genetic lineages with allopatric distributions and variable levels of genetic differentiation (Boumans et al. 2007). Yet, so far, species formation and possible patterns of hybridization between recently diverged chameleon lineages have not been studied in-depth with genome-scale markers, and apart from a study on sex chromosome evolution (Nielsen et al. 2018), and several genome sequencing efforts (e.g., Shylo et al., 2024; Taft et al., 2023; Xie et al., 2023), no phylogenomic study on chameleons is available.

Of the currently 236 nominal species of chameleons (Chamaeleonidae), 42% (100 species) are endemic to Madagascar (Glaw et al. 2025; Uetz et al. 2026;). Malagasy chameleons are classified in the genera *Brookesia, Calumma, Furcifer* and *Palleon* (Klaver & Böhme 1986, 1997; Glaw & Vences 1992, 1994, 2007; Raxworthy et al. 2002; Tolley et al. 2013; Glaw et al. 2013; Glaw 2015), of which *Calumma* is the most species-rich with 44 species (Uetz et al. 2026). *Calumma* species are morphologically diverse, and phenetic species groups (formerly in the genus *Chamaeleo*) were initially distinguished by Brygoo (1971), formalized by Glaw & Vences (1994) and refined by subsequent studies (e.g., Prötzel et al. 2016). Intensified field exploration of Madagascar's remaining primary habitats has led to a large number of discoveries of new species of *Calumma*, often supported by combined morphological and molecular evidence (e.g., Andreone et al. 2001; Raxworthy & Nussbaum 2006; Gehring et al. 2010; Gehring et al., 2012; Prötzel et al. 2018a; Prötzel et al., 2018b, 2020; Glaw et al. 2025).

The informal *Calumma cucullatum* group (Glaw & Vences 1992, 1994) contains species of medium- to large-sized chameleons characterized by large occipital lobes and, often, a single rigid ossified rostral projection in males (Fig. 1). As with other species groups of *Calumma*, the group is based on phenetic similarity and may not represent a monophyletic group; for instance, the phylogenetic estimates of Tolley et al. (2013) suggest that *C. cucullatum* may be more closely related to the species of the *C. furcifer* group (consisting of medium-sized green chameleons mostly without occipital lobes or rostral projections) than to other large species with occipital lobes. The last taxonomic revision of these occipital-lobed chameleons was conducted by Raxworthy & Nussbaum (2006) who described six new species based primarily on evidence from external morphology, thereby elevating the number of recognized species to 12: *Calumma amber* Raxworthy & Nussbaum, 2006, *C. brevicorne* (Günther, 1879), *C. capuroni* (Brygoo, Blanc & Domergue, 1972), *C. crypticum* Raxworthy & Nussbaum, 2006, *C. cucullatum* (Gray, 1831), *C. hafahafa* Raxworthy & Nussbaum, 2006, *C. hilleniusi* (Brygoo, Blanc & Domergue, 1973), *C. jejy* Raxworthy & Nussbaum, 2006, *C. malthe* (Günther, 1879), *C. peltierorum* Raxworthy & Nussbaum, 2006, *C. tsarataananense* (Brygoo & Domergue, 1967), and *C. tsycorne* Raxworthy & Nussbaum, 2006.

The molecular differentiation between lineages of the *C. cucullatum* group has only been assessed in the framework of a large-scale multilocus chameleon phylogeny (Tolley et al. 2013), and in an earlier single-locus mitochondrial phylogeographic study (Boumans et al. 2007). From the available datasets (e.g., Raxworthy & Nussbaum 2006; Glaw & Vences 2007), the distributions of multiple species in the group overlap or abut, suggesting the possibility to recover patterns of hybridization from secondary contacts or late-stage speciation with ongoing gene flow. Several species, in particular *C. brevicorne* and *C. crypticum,* are characterized by a convoluted pattern of mitochondrial lineages (Boumans et al. 2007) of mostly allopatric distribution, differing in color pattern (Glaw & Vences 2007) but less clearly distinct in morphometric or meristic characters. This incongruence in external morphology is difficult to align with current taxonomy and leaves the identification of the species of this phenetic group, and particularly *C. brevicorne* and *C. crypticum*, unreliable, complicating studies of the evolution and phylogeography of the group, as well as the monitoring of the pet trade in *C. brevicorne*, which has a CITES quota of 500 live animals per year (https://www.speciesplus.net, accessed 2025–11-20). Due to these difficulties in characterizing *C. brevicorne* and *C. crypticum*, we herein refer to populations of both taxa as the *C. brevicorne* complex.

Here, we combine various molecular datasets to shed light on the systematics of lineages previously assigned to the aforementioned *C. cucullatum* group. We use a combination of molecular data derived from a variety of sources, including classical Sanger sequencing of mitochondrial and nuclear gene fragments, mitochondrial sequences derived from archival name-bearing types using museomics approaches, and thousands of RADseq-derived single nucleotide polymorphisms (SNPs). We also examine the morphology of a representative set of sequenced voucher specimens. Our data suggest a complex evolutionary history for this group of chameleons, with instances of probable hybridization and mitochondrial introgression, and possible species formation of comparatively shallow lineages in geographical proximity. While a full taxonomic resolution is not yet in reach, our data provide evidence for a new species of occipital-lobed chameleon from northern Madagascar, sister to *C. malthe*, which we formally name and describe in this study.

2. Methods

2.1. Field work and sampling

Specimens and samples of the *C. cucullatum* group were collected between 1996 and 2025 during numerous field expeditions across various regions of Madagascar. Specimens were obtained by opportunistic searching, usually during the night with the aid of flashlights. Representative voucher specimens were anesthetized by intra-coelomic (IC) injection of 250–500 mg/kg pH-neutralized 1% MS-222, and subsequently euthanized by injection of 50% unbuffered MS-222 (Conroy et al. 2009). Tissue samples (leg/ tongue muscle, or liver) were excised and preserved separately in cryovials with 100% ethanol for subsequent long term storage at −20°C, and the specimens were then fixed in 90–100% ethanol and preserved in 70% ethanol. For most samples collected after 2020, saliva swabs were taken in situ and preserved in 99–100% ethanol, and animals were subsequently released at the site of capture.

Voucher specimens were deposited in the collections of the Zoologische Staatssammlung München, Germany (ZSM), the Université d'Antananarivo, Mention Zoologie et Biodiversité Animale, Antananarivo, Madagascar (UADBA), and the Zoologisches Forschungsmuseum Alexander Koenig, Bonn, Germany (ZFMK).

Additional specimens from the Museum National d'Histoire Naturelle, Paris, France (MNHN), the Senckenberg Naturmuseum, Frankfurt, Germany (SMF), and the Natural History Museum, London, UK (BMNH, now NHMUK) were also examined for this study; for the latter, we here assign numbers (of historical types only) under the BMNH acronym to ensure consistency with previous studies. Field numbers of preserved specimens and tissue samples refer to the collections of A. Crottini (ACZC), P.-S. Gehring (PSG), M. Pabijan (MPFC), M. D. Scherz (MSZC), F. Glaw (FGMV, FGZC) and M. Vences (FGMV, MV, ZCMV), D. R. Vieites (DRV), and A. P. Raselimanana (APR).

2.2. Terminology used for supraspecific units

Given that the historical classification of occipital-lobed chameleons does not align with their evolutionary relationships, excacerbated by problems in the unambiguous taxonomic and nomenclatural definition of some species, discussing their relationships is necessarily complex. We here use three different terms to define assemblages of species and lineages:

– Group. This refers to phenetic species groups of Brygoo (1971)

formalized by Glaw & Vences (1994).

– Clade. Within the *C. cucullatum* group, based on our phylogenomic results, we distinguish the *C. brevicorne* clade, the *C. malthe* clade, and the *C. cucullatum* clade.

– Complex. As shown by our results, two species within the *C. brevicorne* clade, *C. crypticum* and *C. brevicorne*, cannot at present be clearly delimited and nomenclaturally defined as our provisional morphological identification are at odds with molecular clusters. We therefore refer to all populations morphologically assignable to either of these two species as members of the *C. brevicorne* complex.

2.3. Morphology

The following morphometric and meristic variables (see Table S1) were measured with a digital caliper to the nearest 0.1 mm, or counted from detailed photographs made of preserved voucher specimens: snout–vent length, measured from snout tip to cloaca and excluding the rostral projection (SVL); tail length, from cloaca to tip of tail (TAL); total length, sum of SVL + TAL; hand length, from hand articulation to tip of claw of longest digit (HAL); foot length from foot articulation to tip of claw of longest digit (FOL); head width at its broadest part, not considering the eyes (HW); horizontal diameter of eye orbit (ED); length of rostral projection projecting beyond snout tip (ROSP); height of rostral projection (HROSP); number of supralabial scales (SUPL); minimum scale count between the eyes, i.e., interocular scales (INTEROC); longitudinal count of ventral scales from mental scale to cloaca, miniature "scales" between normal-sized scales not included (LCVS); number of spines in dorsal crest from behind head to cloaca (SDC); number of spines or spine-like tubercles in gular crest (SGC); vertical count of scales in rostral projection (VSROSP); number of scales on occipital lobe, miniature scales between normal-sized scales not included (SOL); approximate number, and size relative to eye diameter, of enlarged scales on occipital lobes (SOS); periodicity in spine size of dorsal crest present or absent (PSD). With a few exceptions, measurements were taken only from males, to ensure comparability, because more male voucher specimens were available and several sexually dimorphic characters (rostral projection, gular and dorsal crests) are more obvious in males, with stronger differences between species. Mann-Whitney *U* tests of morphological data were carried out in Statistica, version 7. 1 (Statsoft Corp., Tulsa, USA).

2.4. Molecular data sets

For this study, several molecular datasets were assembled and analysed: (1) a dataset comprising concatenated fragments of the three mitochondrial genes: NADH dehydrogenase subunit 2 (ND2), NADH dehydrogenase subunit 4 (ND4), and 16S rRNA (16S) obtained by Sanger sequencing and complemented by sequences derived from several historical type specimens obtained by a museomics approach; (2) an alignment of only the 16S sequences (subset of dataset 1), after excluding sequences with an excessive amount of missing data and trimmed so that all sequences were of similar lengths, for calculation of genetic distances (30 sequences, 454 bp); (3) a trimmed ND4 alignment of 100 samples and 594 bp (subset of dataset 1), used for partition analysis with the program ASAP (Assemble Species by Automatic Partitioning: Puillandre et al. 2021) as our ND4 alignment was the most complete for sample representation; (4) three alignments of DNA sequences of a fragment of the three nuclear-encoded genes for oocyte maturation factor mos, leucine-rich repeat and WD repeat-containing protein, and sacsin (C-MOS, KIAA1239, SACS); (5) a dataset of DNA fragments and single-nucleotide polymorphisms (SNPs) generated by double digestion Restriction site Associated DNA sequencing (ddRADseq, in the following referred to as our RADseq dataset), which was filtered for different sets of ingroups and outgroups to maximize the number of loci available for different analyses; see below. All alignments are available for download from Zenodo (https://doi.org/10.5281/zenodo.18006710). Detailed information on the respective laboratory protocols and analytical methods is given in the following sections.

2.5. Sanger sequencing

We extracted genomic DNA and amplified the gene fragments using standard protocols as described in Glaw et al. (2012) respectively nested PCR protocols from Shen et al. (2012) for KIAA1239 and SACS, using the primers ND2F17 (5′-TGACAAAAAATTGCNCC-3′; Macey et al. 2000) and ALAR2 (5′-AAAATRTCTGRGTTGCATTCAG-3′; Macey et al. 1997) for ND2, ND4 (5′-CACCTATGACTACCAAAAGCTCATGTAGA −3′) and LeutRNA (5′-AGCCATTACTTTTACTTGGATTTGCACC −3′) (originally from Arévalo et al. 1994) for ND4; CO8 (5′-GCTTGGTGTTCAATAGACTGG-3′) and CO9 (5′-TTGGGAGCATCCAAAGTCTC-3′) for C-MOS (Han et al. 2004); KIAA1239-F1 (5′–CARCCTTGGGTNTTYCA–3′), KIAA1239-R1 (5′–CMACAAAYTGGTCRTTR–3′), and internal primers KIAA1239-NF1 (5′–GAGCCNGAYATHTTYTTYG–3′) and KIAA1239-NR1 (5′–TTCACRAANCCMCCNG–3′) (Shen et al. 2012) for KIAA1239; and SACSF2 (5′–AAYATHACNAAYGCNTGYTAYAA–3′) and SACSR2 (5′–GCRAARTGNCCRTTNACRTGRAA–3′) and internal primers SACSNF2 (5′–TGYTAYAAYGAYTGYCCNTGGAT–3′) and SACSNR2 (5′–CKGTGRGGYTTYTTRTARTTRTG–3′) (Shen et al. 2012) for SACS.

We purified PCR products with ExoSAPIT (Thermo Fisher Scientific, Waltham, MA, USA) and sent them for sequencing on an automated capillary DNA sequencer at LGC Genomics (Berlin, Germany). The software CodonCode Aligner version 3.7.1 (CodonCode Corporation) was used to check and correct errors in the DNA sequences based on the chromatograms, and to trim poor-quality stretches and primer sequences from the beginning and end of the sequences. We verified the absence of stop codons in the protein-coding gene fragments (ND2, ND4, C-MOS, KIAA1239, SACS). The new sequences obtained in the present study were submitted to GenBank (accession numbers PZ367831–PZ367833, PZ373022–PZ373357, PZ379204–PZ379207). A full table with all sequences used, accession numbers and metadata is available from Zenodo (https://doi.org/10.5281/zenodo.18006710).

2.6. Museomics

Name-bearing types of five *nomina* in the *C. cucullatum* group were sampled for DNA sequencing using a museomics (Fong et al. 2023) approach, i.e., archival DNA sequencing of the holotypes of *Chamaeleon brevicornis* Günther, 1879 (BMNH 1946.8.21.41), *Chamaeleon cucullatus* Gray, 1831 (BMNH 1946.8.21.82), *Chamaeleon gularis* Günther, 1879 (BMNH 1946.8.21.50), *Chamaeleon malthe* Günther, 1879 (BMNH 1946.8.21.47) (see Campbell & Denzer 2019), and *Chamaeleo brevicornis tsarafidyi* Brygoo & Domergue, 1970 (MNHN-RA 1993.172). Samples were taken in 2023 at the NHMUK and 2025 at the MNHN, sampling each type specimen for a small piece of thigh muscle tissue after inflicting a small incision and reflecting the ventral skin of the thigh. To maximize success, we aimed to obtain a minimum of 5 mg of muscle tissue per specimen, since smaller amounts have resulted in low success rates for yielding any endogenous DNA (own, unpublished data). Sampling was done with sterile scalpels, scissors and tweezers, and the samples stored in vials of pure ethanol. Prior to DNA extraction, each sample was weighed and incubated in a Guanidine Thiocyanate (GuSCN)-based extraction buffer solution, adapted from Rohland et al. (2004), at 37°C overnight. The next day, a total of 25 µl DNA extract for every sample was gained from the supernatant through the extraction treatments described in Straube et al. (2021) based on the ancient DNA extraction protocol specified in Dabney et al. (2013). The yield of DNA was quantified based on 1 µl of DNA extract using the Qubit dsDNA HS Assay Kit 0.2–100 ng/µl (Life Technologies, Carlsbad, California, US) according to the instructions of the manufacturer. Subsequently, single-stranded library preparation was carried out following the protocol of Gansauge et al. (2017). Lab work was conducted in a dedicated DNA facility at the University of Potsdam, Germany, which meets all

requirements for work with historical samples (see Fulton & Shapiro 2019) and extraction and library blanks were run alongside all samples to check for contamination. Final library concentrations and fragment length distributions were assessed using a 2200 TapeStation (Agilent Technologies) assay. Sequence data was obtained through shotgun-sequencing of approximately five million (*C. b. tsarafidyi*) or one million (the other four types) 75-bp single-end reads using an Illumina Nextseq 500/550 sequencing platform at the University of Potsdam, following the procedure described in Paijmans et al. (2017). The quality of the obtained reads was visualized twice using FastQC (https://www.bioinformatics.babraham.ac.uk), both before and after trimming of Illumina adapter sequences and discarding reads shorter than 30 bp with cutadapt v1.12 (Martin 2011).

We used local Blast (Blast+; Camacho et al. 2009) as implemented in BlasTax (Vences et al. 2026), which is part of the iTaxoTools bioinformatic platform (Vences et al. 2021), against a library of ND4, ND2 and 16S sequences of all main genetic lineages of the *Calumma brevicorne* complex, and collected the matching reads in a fasta file. We then used CodonCode Aligner version 3.7.1 (CodonCode Corporation) to map the matching reads separately to reference sequences of all *C. brevicorne* complex lineages (option: "align to reference"), verified the resulting assemblies were congruent (thus, no reference bias was introduced), and used the most complete consensus sequences obtained as representing the respective type specimens, with missing sections in-between partial contigs coded by the letter "N".

2.7. Mitochondrial DNA phylogeny, genetic distances and molecular diagnosis

Sequences of all three mitochondrial gene fragments (ND2, ND4, 16S), including sequences of these gene fragments obtained from the five name-bearing types, were concatenated after MAFFT alignment (Katoh & Standley 2013) with the G-INS-i option as implemented in Concatenator (Vences et al. 2022). The final concatenated alignment length was 2,264 bp (16S: 454 bp, ND4: 721 bp, ND2: 1,089 bp).

The concatenated alignment was used to infer a Maximum Likelihood (ML) tree using IQ-Tree v.2.4.0 (Minh et al. 2020), using the best substitution models and data partitions identified using ModelFinder (Kalyaanamoorthy et al. 2017) and 2,000 full non-parametric bootstrap replicates. We used a partitioning scheme by gene (not by codon) to avoid overparametrization, given the relatively short length of the fragments used.

Uncorrected pairwise genetic distances were calculated from the trimmed 16S alignment (454 bp) using MEGA7 (Kumar et al. 2016). Detailed distance tables and treefiles are available on Zenodo (https://doi.org/10.5281/zenodo.18006710).

2.8. Genealogy inferred from nuclear-encoded gene sequences

We analysed mitochondrial and nuclear data separately from each other rather than concatenating them, because a concordant signal of markers with different modes of inheritance (nuclear and mitochondrial) provides additional support for distinct evolutionary lineages under the genealogical concordance species criterion (Avise & Ball 1990). For our nuclear alignments (C-MOS, KIAA1239, SACS), we used a genealogy visualization approach to represent the relationships among alleles (haplotypes) graphically. Alignments were manually trimmed by removing regions of poor quality and sequences with missing data so that all sequences per alignment were of equal length. Alleles were inferred using the PHASE algorithm (Stephens et al. 2001) implemented in the software Hapsolutely (part of iTaxoTools) (Vences et al. 2021, ; Vences et al., 2024), and haplotype genealogies were visualised based on the Fitch tree algorithm (Salzburger et al. 2011; Matschiner, 2016) in the same program.

2.9. ddRADseq dataset

A total of 77 samples of all currently recognized species and all major lineages in the *C. cucullatum* group, plus a set of hierarchical outgroups, were selected for double digestion restriction site associated DNA sequencing (ddRADseq). Library preparation was adapted from Brelsford et al. (2016), as fully described in Dufresnes et al. (2025). In summary, it consisted of restriction enzyme digestion with MseI and SbfI, ligation of adapters with individual unique barcodes for each sample, PCR amplification, and a size selection step of the ligated fragments (between 400 and 500 bp) by performing a gel electrophoresis and extraction using the Monarch DNA Gel Extraction Kit (New England Biolabs). Samples were prepared in two separate library pools (each also featuring other samples) and sequenced paired-end on an Illumina NextSeq (2 x 75 bp kit) or (for three additional samples) a partial lane of an Illumina Novaseq (2 x 150 bp kit).

Raw reads were demultiplexed and *de novo* assembled and filtered with Stacks v2.61 (Catchen et al. 2013; Rochette et al. 2019). All reads were trimmed to 65 bp (module *process_radtags*). Assembly and SNP calling for downstream analyses used *denovo_map.pl* and *populations*, respectively. The final Stacks assembly contained 629,515 loci with a mean effective per-sample coverage of 41.0x. Default stacking parameters (−m, −n and −M) were applied, following suggestions from Paris et al. (2017). These data were subsetted for specific downstream analyses to meet model assumptions regarding missing data. Loci were filtered with respect to the number of individuals for which a locus must be present (−p) and optimized to retain the maximum number of loci while minimizing missing data across the species included. We also applied (across the entire set of 77 samples) a minimum allele frequency (−min-maf) threshold of 0.05 to limit PCR duplicates, and a maximum-observed heterozygosity (−max-obs-het) threshold of 0.75 per locus to limit paralog overmerging.

For phylogenetic analyses, we used two concatenated alignments of the RADseq-derived data: (1) one including all 77 samples (71 *Calumma* + 6 *Furcifer* as outgroup), featuring 1,643 RAD loci (219,880 bp, 8,135 SNPs) with each sequenced for at least 67 samples; and (2) one restricted to the 61 samples of the "*C. brevicorne* clade" and "*C. malthe* clade" (+ 1 *C. vencesi* as outgroup), which allowed inclusion of more loci and SNPs: 3,546 RAD loci (480,133 bp, 13,666 SNPs) with each sequenced for at least 55 samples. ML phylogenies were reconstructed using IQTree v2.2.0 (Minh et al. 2020). The best substitution model for each dataset was determined using the integrated ModelFinder (Kalyaanamoorthy et al. 2017), and branch support was assessed through 1,000 ultrafast bootstrap replicates (UFBoot; Hoang et al. 2018). Final trees were rooted and visualized using a custom R script (available from https://doi.org/10.5281/zenodo.18006710).

In addition to the concatenation approach, we also estimated a species tree by multispecies coalescent analysis using SNAPPER (Stoltz et al. 2021), implemented in BEAST 2 (Bouckaert et al. 2019), version 2.7.7. The input XML file was generated in BEAUti v2.7.7, part of the BEAST package, from a VCF file containing 8,142 SNPs of which each position was genotyped in at least 67 of the 77 samples (Stacks populations parameter p = 67). Samples were assigned to 26 groups corresponding to the sampled species and the identified *C. malthe* and *C. brevicorne* phylogroups (BRE1–BRE7, MA1–MA3). We applied a Yule tree prior with gamma-distributed priors on both the birth rate ($\alpha = 2.0$, $\beta = 200$) and the coalescent rate ($\alpha = 0.01$, $\beta = 100.1$). A subset of 965 SNPs, all genotyped in at least one individual per predefined group, were informative for the analysis. A single Markov chain was run for 1.5 million iterations, with parameters sampled every 1,000 iterations. Convergence was assessed in Tracer v1.7.2 (Rambaut et al. 2018), and tree set variation was visualized for explorative examination using DensiTree (Bouckaert 2010). A maximum clade credibility tree was generated with TreeAnnotator after discarding the first 10% of samples as burn-in.

2.10. Analyses of population structure

Patterns of population structure and admixture among subgroups were estimated for various partitions of our SNP data, following the same filtering strategy as above but considering only one SNP per locus (−write-single-snp flag in Stacks) to avoid physically linked loci, as a prerequisite of clustering analyses which assume no linkage disequilibrium between loci. Specifically, these datasets were as follows: (1) 3,017 SNPs for 60 samples in the *C. cucullatum* group (each scored for at least 55 samples); (2) 3,845 SNPs for 41 samples belonging to the "*brevicorne* clade" (each genotyped in at least 37 samples); (3) 5,212 SNPs for 19 samples belonging to the "*malthe* clade" (herein referred to as MA samples; each scored for all 19 samples of this clade); (4) 5,027 SNPs for 25 samples belonging to the "*brevicorne* complex" subgroup (herein referred to as BRE samples; each scored for at least 22 samples); (5) 5,211 SNPs for 32 samples belonging to the "*brevicorne* complex" and to the subgroup composed of *C. jejy/peltierorum* (each scored in at least 28 samples). For each dataset, we performed a preliminary assessment of population structure and admixture estimated with STRUCTURE v.2.3.4 (Pritchard et al. 2000, Falush et al. 2003), using the admixture model without sample pre-assignment (locprior), correlated allele frequencies, inferring lambda, and setting the mixing to 1 (which helps convergence for high K values with large SNP datasets). In each analysis, we explored $K = 2$–10, (using up to 20 replicates, each consisting of 20,000 burnin followed by 20,000 iterations).

Because the primary objective of this analysis was to assess contemporary admixture among the lineages identified in the phylogenetic analyses (see Results), we prioritized clustering solutions that effectively distinguished these lineages rather than attempting to infer a single statistically "optimal" number of clusters (K). The notion of an "optimal K" can be contentious as it is relative to the scale and goal of the analyses, and the processes generating genetic structure structure (e.g., deep phylogeographic divergence, recent population fragmentation, isolation-by-distance). Its identification may be further biased by methodological considerations, such as uneven sampling among lineages/putative clusters, as in our dataset. Instead, we evaluated results across a range of K values and retained runs that (i) maximized log-likelihood, (ii) minimized alpha values, and (iii) maximized F_{st} among each K. Maximizing log-likelihood ensures that the model provides the best statistical fit to the observed genetic data under the assumed number of clusters. Minimizing the alpha parameter (which reflects the degree of admixture) favors solutions in which individuals are primarily assigned to a single cluster, thereby reducing spurious signals of widespread admixture. Finally, maximizing ingroup F_{st} promotes clustering configurations that enhance genetic differentiation among inferred groups, ensuring that clusters represent meaningful structure rather than weakly differentiated or artifactual ("ghost") groupings that can arise with large SNP datasets.

2.11. ABBA-BABA tests

To assess the prevalence of historical gene flow across the phylogeny, we calculated f-statistics from the 77-sample dataset using ABBA–BABA tests. These tests evaluate whether one of two sister lineages (P1 and P2) shares an excess of derived alleles with a more distantly related lineage (P3). Analyses were conducted using the Dtrios function implemented in Dsuite v0.5 r58 (Malinsky et al. 2021), applying a block jackknife with a block size of 1. The input topology was derived from the Maximum Likelihood tree previously calculated with IQ-TREE for the 77-sample dataset, and collapsed to a single tip per species or phylogroup using a custom R script. To summarize patterns of gene flow across the phylogeny, f-branch statistics were calculated with the Fbranch function in Dsuite, and the script dtools.py (distributed with the software) was used to generate f-branch plots.

2.12. Species delimitation and species delimitation rationale

To delimit new species, we follow the general lineage concept (de Queiroz 1998, 2007) in combination with a relaxed biological species criterion, i.e., demanding reproductive isolation indicated by restricted gene flow among lineages (e.g., Speybroeck et al. 2020; Dufresnes et al. 2021). Since reproductive barriers generated through time can increase population divergence and signal agreement among unlinked loci (Avise & Wollenberg 1997), we use genealogical concordance (Avise & Ball 1990) between mitochondrial and nuclear loci, especially in populations occurring in sympatry or close geographical proximity, as a potential indication of restricted gene flow. Using a combination of genetic and morphological evidence, we then assign tentative species status to lineages (Padial et al. 2010).

In the absence of hybrid zone data (Dufresnes et al. 2021) for species of the *C. cucullatum* group, we first used ASAP (Puillandre et al. 2021) on the largest mitochondrial data partition (ND4, 594 bp) to computationally determine primary mitochondrial partitions (i.e., partitioning the samples into subsets, i.e. mitochondrial lineages that represent primary species hypotheses, PSCs).

For the focal taxa in the *C. brevicorne* complex, and populations assigned to *C. malthe*, we also performed multispecies coalescent (MSC)-based lineage delimitation analyses using BPP v4.8.7 (Flouri et al. 2018) on the RADseq data. This method estimates posterior probabilities of lineage splits (putative speciation events) among predefined groups under the multispecies coalescent. Individuals were partitioned into groups which (i) were monophyletic (i.e. phylogroups) in our concatenation ML tree and (ii) in most cases also represented a cluster in one of the STRUCTURE analyses. Most, but not all, of these groups coincided with the subsets identified by ASAP from the mitochondrial sequences. Three groups were defined for *C. malthe* (MA1, MA2, MA3), and six groups for the *C. brevicorne* complex (BRE1, BRE2, BRE3, BRE5, BRE5b, BRE7). The dataset for *C. malthe* included 6,840 loci sequenced in all 22 samples, the dataset for the *C. brevicorne* complex included 6,036 loci sequenced in at least 22 of the 25 samples included. Input files were generated from the -fasta-samples output of Stacks populations using a custom R script. We implemented the A11 model, which jointly estimates lineage delimitation and phylogeny, with priors on population size (θ) and divergence time (τ) set to 0.002. The topology inferred with IQ-TREE was used as the starting tree. A Markov chain Monte Carlo (MCMC) analysis was run to obtain 10,000 samples, with a sampling frequency of 10 and a burn-in of 2,000 iterations. To evaluate sensitivity to prior assumptions, we repeated the analyses using alternative prior values of 0.02 (reflecting larger population sizes and deeper coalescence times) and 0.005 (reflecting smaller population sizes and shallower coalescence times).

The lineages or clusters (subsets) identified by ASAP and BPP were then manually examined for concordance with clustering in STRUCTURE analyses, for absence of haplotype sharing among subsets in the three Sanger-sequenced protein-coding nuclear loci C-MOS, KIAA1239, and SACS, for differences in morphological characters, and for geographic separation (i.e., cases of geographical co-occurrence without admixture). The possible species status of subsets was then evaluated and discussed taking the combined evidence into account.

2.13. Initial species identification of samples

Collected samples and voucher specimens were preliminarily assigned to species in the field based on (i) their external morphology and (ii) geographic location. Adult males characterized by relatively small body size (usually less than 116 mm in snout–vent length), short rostral projection < 2.5 mm, vertically often made up by maximally two scales) roughly conform with the definition of *C. crypticum* of Raxworthy & Nussbaum (2006) and Glaw & Vences (2007), while males of larger size (> 116 mm in snout–vent length), three or more vertical scales in rostral projection, and rostral projection length > 3 mm fit with

C. brevicorne as currently defined. Additional samples of females and juveniles from the same populations were tentatively assigned to the same species. Field identification of some other locally restricted species (e.g., *C. amber, C. hilleniusi, C. jejy*) was based primarily on their collection locality, while other species such *as C. cucullatum, C. malthe, C. peltierorum, C. tsaratananense* and *C. tsycorne* could be unambiguously identified based on their morphology.

2.14. Nomenclatural acts

The electronic edition of this article conforms to the requirements of the amended International Code of Zoological Nomenclature, and hence the new names contained herein are available under that Code from the electronic edition of this article. This published work and the nomenclatural acts it contains have been registered in ZooBank, the online registration system for the ICZN. The LSID (Life Science Identifier) for this publication is: urn:lsid:zoobank.org:pub:FB4FD4BE-07DD-42A8-B1D4-FD88ED6D79AF. The electronic edition of this work was published in a journal with an ISSN, has been archived and is available from the CLOCKSS digital repository.

3. Results and discussion

3.1. Phylogenomic evidence for paraphyly of the C. cucullatum group

Our final dataset with outgroup taxa included 1,643 loci derived from the ddRADseq data, resulting in an alignment length of 219,880 bp. The ML tree inferred from this data was well-resolved, with most nodes receiving maximum bootstrap support (Fig. 2; Fig. S1). In line with Tolley et al. (2013), the tree suggests non-monophyly of the included occipital-lobed chameleons (*C. cucullatum* group): *C. cucullatum* was placed sister to the *C. furcifer* group, and *C. malthe* was sister to a clade containing species of the *C. nasutum* group and all other species of the *C. cucullatum* group. Both aspects had been previously found in a multilocus phylogeny based on three nuclear-encoded and three mitochondrial gene fragments (Tolley et al. 2013), thus firmly establishing polyphyly of the phenetic *C. cucullatum* group. A similar topology was recovered by a species tree analysis (Fig. S2) which, however, differed from the concatenation tree (Fig. 2) by placing *C. hilleniusi* nested within the *C. brevicorne* complex, and the two species of the *C. nasutum* group sister to a clade made up by *C. hafahafa* and *C. tsaratananense*.

In the following, we will focus on results and discussion of evolutionary relationships of occipital-lobed chameleons in the *C. brevicorne* clade (including *C. amber, C. brevicorne* and *C. crypticum* [both of the latter taxa here considered as part of the *C. brevicorne* complex], *C. hafahafa, C. hilleniusi, C. jejy, C. peltierorum*, and *C. tsaratananense*) and in the *C. malthe* clade as defined herein (Fig. 2), and analyse genetic structure separately within these clades. We label lineages identified by our various clustering and lineage delimitation analyses within the *C. brevicorne* complex as BRE1–BRE7 and within *C. malthe* sensu lato as MA1–MA3.

A Maximum Likelihood tree including all 60 ingroup samples of the *C. brevicorne* and *C. malthe* clades with *C. vencesi* as an outgroup, (3,546 loci and an alignment of 480,133 bp featuring 13,666 SNPs) (Fig. 3), largely agreed in topology with the more inclusive *Furcifer*-rooted tree including all samples but fewer loci. Most species of occipital-lobed chameleons were resolved as deep and monophyletic lineages, i.e., *C. amber, C. hafahafa, C. hilleniusi, C. tsaratananense*, with full bootstrap support in all cases where two or more samples were included. As an exception, *C. peltierorum* was only relatively shallowly divergent from the morphologically highly divergent *C. jejy*. The phylogenomic data also supported a clade with all specimens of *C. malthe* sensu lato (BS = 100%), with two fully supported lineages corresponding to (i) the mitochondrial lineages MA1 and (ii) MA2 + MA3 (see below).

For chameleons of the *C. brevicorne* complex, our results suggest extensive admixture and do not show a clear divergence between individuals assigned to either *C. brevicorne* or *C. crypticum* by our provisional morphological and geographical identification. According to our morphological and geographical data (Table S1) and those of Raxworthy & Nussbaum (2006), all individuals from Andasibe are assignable to *C. brevicorne* and formed a clade together with two individuals from Anjozorobe (BRE5); other populations assignable to *C. brevicorne* from Ranomafana and Andringitra were in BRE2/3; while populations provisionally assignable to *C. crypticum* based on morphology and geography (Mandraka, Andohahela, and the northern localities Tsaratanana and Bemanevika) clustered in three genetic lineages (BRE1, BRE5b, BRE7) which did not form a monophyletic group in the tree. BRE1 was nested in a clade with BRE2/3 and BRE5, while BRE5b and BRE7 successively split off from the nodes leading to these clades. To add to this conundrum, within populations morphologically assignable to *C. brevicorne*, specimens in BRE5 have a very different color from those in lineage BRE2/3 (Glaw & Vences 2007 and Fig. 1 herein); in fact BRE2/3 males with their distinct blue pattern in breeding color rather resemble males of BRE1 and BRE5b. Together with nomenclatural uncertainty arising from the unexpected phylogenetic position of the type specimen of *Chamaeleo brevicornis* Günther, 1879 in the mitochondrial tree (see below) this supports our decision to subsume all *C. brevicorne* and *C. crypticum* individuals in the *C. brevicorne* complex (Fig. 3) until future in-depth study can resolve their taxonomy.

3.2. Museomics

Four historical types included in the museomics analysis and shotgun-sequenced for a target of ca. one million reads yielded 90–611 reads per mitochondrial DNA fragment matching to the reference sequences (Table 1). The holotype of *C. b. tsarafidyi* was sequenced for five million reads and yielded only 20–49 matches, but the assembled sequences were sufficient to reliably infer the phylogenetic position of this, as well as all other specimens, in the mitochondrial tree (Fig. 4). Numbers of matches were at similar orders of magnitude for each gene fragment (16S, ND2, ND4), with slightly larger numbers for the protein-coding ND2 and ND4 (Table 1), which may be explained by longer reference sequences for these genes.

3.3. Mitochondrial phylogeny

The ML tree inferred from 2,264 bp of the three concatenated mtDNA fragments (Fig. 4) placed both *C. cucullatum* (here used as the outgroup, based on findings from the phylogenomic analysis; Fig. 2) and *C. tsycorne* as deeply divergent lineages, clearly separated from all other ingroup taxa. Within the 112 ingroup samples, the mitochondrial phylogeny confirmed most currently accepted species as monophyletic lineages, i.e., *C. amber, C. hafahafa, C. hilleniusi,* and *C. tsaratananense,* supported by high bootstrap values (BS = 99–100%). Specimens classified as *C. peltierorum* were paraphyletic, with sequences from Marojejy (BS = 100%) being sister to those from the Tsaratanana/Bemanevika/Ampotsidy area plus *C. jejy* (BS = 100%). The lowest genetic distances in the 16S fragment were found between *C. jejy* and *C. tsaratananense* (1.3%), *C. peltierorum* and *C. tsaratananense* (1.8%), and *C. jejy* and *C. hafahafa* (2.2%).

Our analysis is the first to include molecular data for *C. tsycorne*, and places this species splitting from a deep node, sister to the clade of all ingroup species. The very long branch connecting this species may indicate that it does not belong to the *C. cucullatum* group at all, similar to *C. capuroni* which according to Tolley et al. (2013) turned out to be sister to the *C. parsonii* group, in agreement with hemipenial data (Brygoo 1978). This further suggests the need for a revision of the species groups within *Calumma*.

A highly complex phylogenetic topology was revealed for *C. malthe sensu lato*, which consisted of three deep phylogenetic lineages here named MA1–MA3: lineage MA1 included samples from localities in the Northern Central East, as well as the *C. malthe* holotype based on

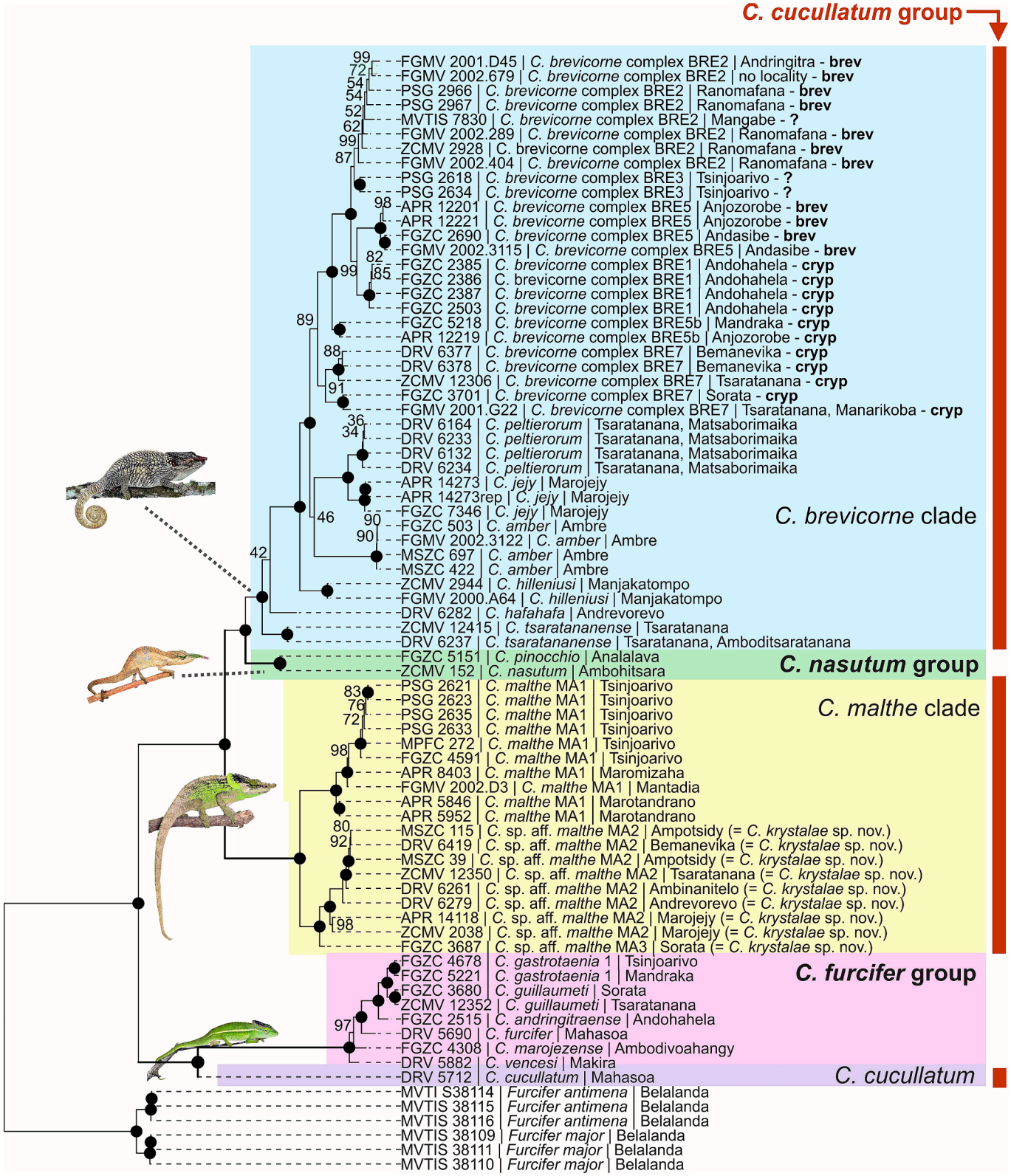

Fig. 2. Maximum Likelihood tree showing paraphyly of the informal phenetic *Calumma cucullatum* group of occipital-lobed chameleons, relative to representatives of the *C. nasutum* and *C. furcifer* groups. The tree is based on 77 samples and 1,643 ddRADseq loci, totalling 219,880 bp (8,135 SNPs). Black dots indicate 100% support from 1,000 replicates of ultrafast bootstraps (numbers shown where < 100%). Samples of *Furcifer antimena* and *F. major* were used as outgroups. Inset photos show representative individuals of the respective clades and species groups (*C. brevicorne, C. pinocchio, C. malthe,* and *C. gastrotaenia*). Vertical red bars mark the species traditionally included in the *C. cucullatum* group, which the tree confirms as non-monophyletic with respect to other species groups without occipital lobes. Boldface labels **cryp** and **brev** in tip labels indicate tentative morphological identification of the specimens in the *C. brevicorne* complex.

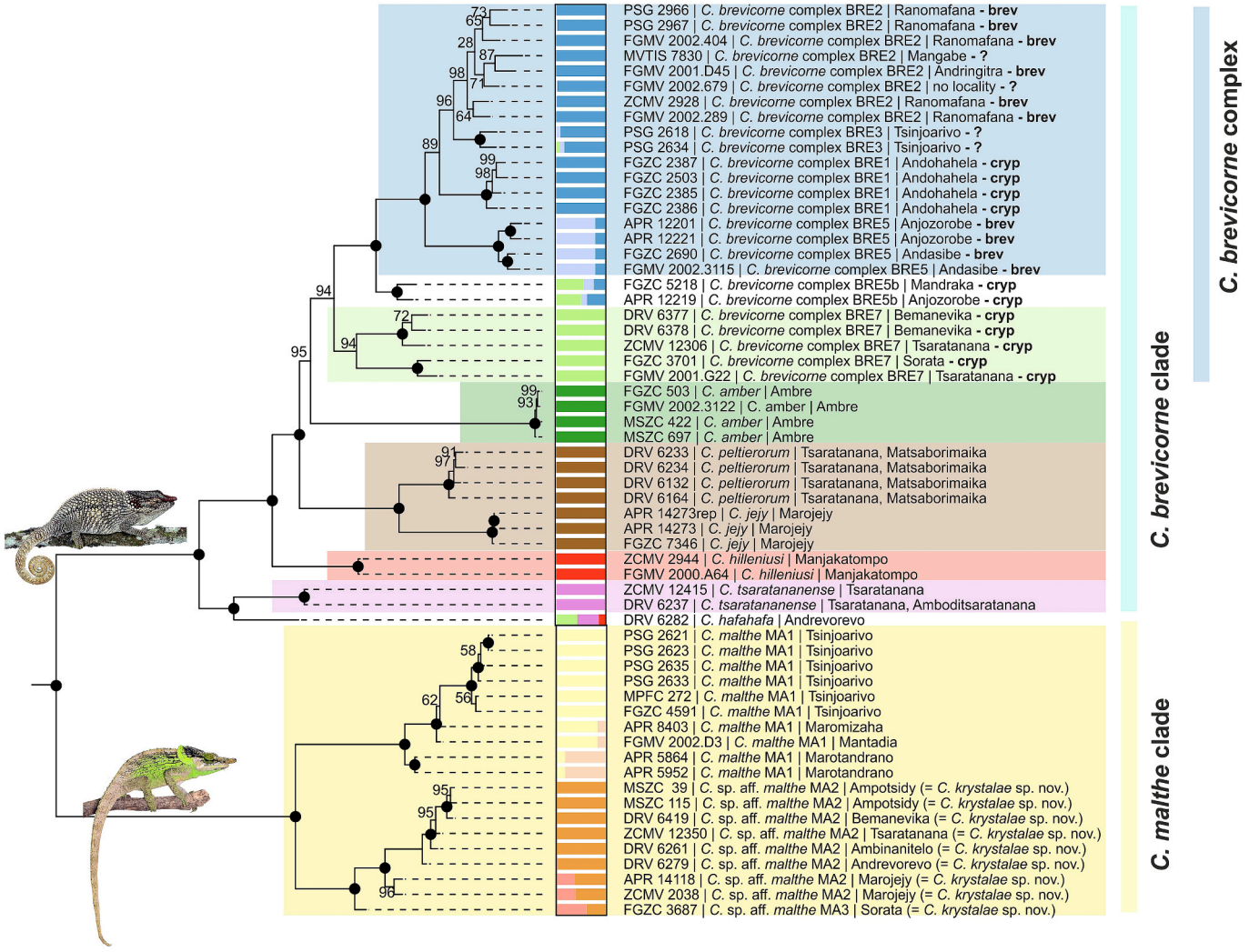

Fig. 3. Maximum Likelihood tree of 60 samples of the *Calumma brevicorne* clade and *C. malthe* clade of occipital-lobed chameleons, based on 3,546 loci derived from RADseq, totalling 480,133 bp (13,666 SNPs). The tree is rooted by *C. vencesi* (not shown). Black dots indicate 100% support from 1,000 replicates of ultrafast bootstraps (numbers shown where < 100%). Boldface labels **cryp** and **brev** in tip labels indicate tentative morphological identification of the specimens in the *C. brevicorne* complex. Barplots show assignment probabilities to the highest number of genetic clusters retrieved by Bayesian clustering with STRUCTURE, conducted separately for the *C. brevicorne* (3,895 SNPs, K = 7) and *C. malthe* clades (5,212 SNPs, K = 4). Inset photos show representative individuals of the *C. brevicorne* clade and the *C. malthe* clade (see Fig. 1).

museomics sequences; MA2 included the northern localities Marojejy, Ampotsidy, Tsaratanana, Bemanevika, Andrevorevo; and MA3 included samples from Sorata, the northernmost site. Strikingly, the three *C. malthe* mtDNA lineages were not recovered as monophyletic group in the mitochondrial analysis, despite jointly forming the *C. malthe* clade in the phylogenomic trees (Figs 2–3): instead, in the mitochondrial tree, MA1 was sister to the entire clade of the other species (BS = 77%) while the position of MA2 and MA3 was unresolved. 16S distances between the three *malthe* lineages were 4.3–4.7%.

As in the phylogenomic tree (Fig. 3), the mitochondrial tree (Fig. 4) did not reveal two clades in the *C. brevicorne* complex that could unambiguously be interpreted as corresponding to the species *C. brevicorne* and *C. crypticum*. Instead, up to seven deep mitochondrial lineages (BRE1–BRE7) could be distinguished: lineage BRE1 from the South East, including samples from Andohahela and Ambositra; BRE2 from the Southern Central East, including samples from Ranomafana and Andringitra, and the *brevicorne* holotype; BRE3 from Tsinjoarivo; BRE4 from Itremo; BRE5 from the Northern Central East, including among others, all samples from Andasibe, Mantadia, Anjozorobe, Ambohitantely (type locality of *crypticum*), and Mandraka, also including the museomics sequence of the holotype of *gularis*; BRE6 from Fierenana in the Northern Central East, and BRE7 from various sites in northern Madagascar such as Makira, Bemanevika and Analabe. While BRE1–BRE6 formed a well supported clade (BS = 90%), BRE7 was placed in a clade with other species such as *C. amber* and *C. peltierorum* (BS = 93%). 16S distances between BRE1–BRE6 were 1.1–2.4%.

The ASAP analysis suggested two species partitions based on the mitochondrial data sets, one with 16 and one with 32 subsets, with equally low ASAP score (4.0). The more realistic 16-subset partition separated all species except *C. jejy* (merged with *C. peltierorum*), and distinguished the lineages MA1–MA3, as well as BRE1 + BRE5 (despite these two clusters not being sister to each other in the tree; Fig. 4), BRE2, BRE3 + BRE4, BRE6 and BRE7.

3.4. Mito-nuclear discordance, hybridization and introgression

Our findings of discordance between the mitochondrial and RADseq phylogenies may indicate events of mitochondrial introgression, both in the *C. brevicorne* clade and the *C. malthe* clade. This is most obvious in lineage BRE7, which forms a distinct lineage that is not directly related to the *C. brevicorne* complex in the mtDNA tree, but is instead recovered as sister to the other populations of the *C. brevicorne* complex in the

Table 1
Numbers of Illumina reads matching reference sequences of holotypes of *Calumma* for the three mitochondrial target genes (16S, ND2, ND4). Numbers are numbers of unique reads compared by BLAST to a database containing sequences of equal length of the mitochondrial lineages to which the respective types belong.

Nomen	Catalogue number	Total reads	Reads 16S	Reads ND2	Reads ND4
Chamaeleon brevicornis Günther, 1879	BMNH 1946.8.21.41	552,995	101	103	93
Chamaeleon gularis Günther, 1879	BMNH 1946.8.21.50	1,027,410	553	1,616	908
Chamaeleo brevicornis tsarafidyi Brygoo & Domergue, 1970	MNHN-RA 1993.172	4,072,962	28	49	20
Chamaeleon malthe Günther, 1879	BMNH 1946.8.21.47	773,979	413	813	611
Chamaeleon cucullatus Gray, 1831	BMNH 1946.8.21.82	1,042,980	88	256	144

phylogenomic dataset, to which it is further more congruent in morphology. The mitochondrial data furthermore reveal at least one case of mito-nuclear discordance between *C. brevicorne* lineage BRE7 and *C. peltierorum*, both of which co-occur in the wider Tsaratanana region in northern Madagascar: specimen ZCMV 12306 has a *peltierorum* mitochondrial genome but is placed confidently with *C. brevicorne* BRE7 by the phylogenomic data. STRUCTURE analyses including the *C. brevicorne* complex and *C. peltierorum/C. jejy* did not provide clear indications of admixture when five groups are allowed; however, all BRE7 specimens appeared to have substantial assignment probabilities to *C. peltierorum* when constraining the analyses to the two main groups (Fig. 5). Furthermore, samples from Andasibe and Mantadia (based on morphology identified as *C. brevicorne*), Mandraka (morphologically identified as *C. crypticum*), and Ambohitantely (type locality of *C. crypticum*) in the mitochondrial tree are all part of lineage BRE5, but in the phylogenomic tree, the Mandraka sample (along with one sample from Anjozorobe labelled as BRE5b) has a position distant from the Andasibe sample. Finally, in the *C. malthe* clade, the mitochondrial data suggest non-monophyly of the three lineages MA1, MA2, and MA3, while the phylogenomic data place all respective samples in a strongly supported monophyletic group.

We hypothesize that some of these cases are probably best explained by complex scenarios of ancestral introgressive hybridization with mitochondrial capture, which in the current sampling design are not obviously detectable as admixture signals in the STRUCTURE analyses (a method better able to detect recent introgression: Pang & Zhang 2025). The ABBA-BABA analyses revealed an excess of shared derived alleles for several of the lineages affected by mito-nuclear discordance (see *f*-branch matrix in Fig. S3). The highest f_b values involved BRE7, indicating strong excess allele sharing with *C. peltierorum* ($f_b = 0.205$) and BRE5b ($f_b = 0.299$), consistent with introgression involving these lineages or their ancestors. Additional signals were detected between BRE5b and BRE5 ($f_b = 0.220$), and between BRE2 and BRE1 ($f_b = 0.194$). In contrast, the ABBA-BABA tests did not find indications for introgression among lineages MA1–MA3, or between any of those and other species, suggesting that the mito-nuclear discordance observed for *C. malthe* may be due to other factors such as ILS, or by an incorrectly resolved mitochondrial phylogeny.

A more thorough analysis of the distribution and extent of these cases of putative admixture and introgression, especially of the *C. brevicorne* complex along the almost 500 km gap between the occurrences of BRE5 and BRE7, will require a denser geographical sampling in future studies to identify and characterize their hybrid zones (Fig. 5).

From an evolutionary perspective, the processes underlying the apparently widespread mitochondrial introgression in these chameleons are intriguing and may in part include adaptive drivers such as fixation of introgressed haplotypes driven by metabolic constraints (Toews & Brelsford 2012; Bonnet et al. 2017). Most species and lineages in the *C. brevicorne* clade can be found at elevations up to > 1,500 m above sea level, and some species such as *C. jejy, C. peltierorum* or *C. tsaratananense* occur regularly at elevations above 2,000 m a.s.l.. Whether adaptation of mitochondrial haplotypes to cold montane habitats can be invoked to have favored some of the observed introgression events, such as that of a *C. peltierorum* haplotype into lineage BRE7 of the *C. brevicorne* complex, might be worth testing in future studies.

Another case where mitochondrial introgression might be suspected is the species pair *C. jejy* and *C. peltierorum*. These two species have relatively shallow mitochondrial divergences but differ by various striking morphological differences, especially by males of *C. peltierorum* having bluish lateral color (unknown in *C. jejy*), distinct rostral projection (absent in *C. jejy*), and large spines in dorsal and ventral crests (less developed in *C. jejy*) (Fig. 1). However, several morphological similarities (well-developed gular crest, heterogeneous scales on body and limbs) as well as their firm placement as sister species in the phylogenomic analysis with equally shallow divergence (Figs 2–3) suggest that their mitochondrial similarity is not a result of introgression but reflects relatively recent species formation. These two species are, as far as we know, fully allopatric, with *C. jejy* being restricted to the summit of the Marojejy Massif; this argues against a scenario where ongoing gene flow would homogenize their genomes except at the loci controlling morphology. We therefore hypothesize that these species speciated relatively recently, followed by rapid morphological evolution.

3.5. Assessment of species boundaries and taxonomy in the C. brevicorne complex

The molecular and morphological data available suggest that a two-species classification (*C. brevicorne* and *C. crypticum* sensu Raxworthy & Nussbaum 2006) may not correctly reflect the genetic and morphological diversity of the *C. brevicorne* complex. Importantly, given the mito-nuclear discordance detected in these chameleons, delimiting species based on monophyletic groups in the mitochondrial tree is inherently unreliable and the subsets suggested by the ASAP analysis do not provide reliable primary species hypotheses. In addition to well-known sources of gene tree discordance—such as incomplete lineage sorting, standing genetic variation, convergent molecular evolution, and phylogenetic error due to missing data (e.g., Steenwyk et al. 2023)—our chameleon phylogeny may also be influenced by introgression attraction *sensu* Karin et al. (2025). In lineages with recurrent historical admixture, this process can lead to species being resolved as non-monophyletic even in phylogenomic analyses by incorporating alleles derived from past introgression events (Karin et al. 2025; Gippner et al. 2024).

Given the indications for hybridization and introgression in the *C. brevicorne* complex, it would be appealing to consider all populations as a single species, *C. brevicorne*, subdivided into allopatric populations for which some authors would advocate using subspecies status (Dufresnes et al. 2023). Our data are insufficient to fully reject this scenario, but provide evidence against it from the samples from Anjozorobe included in the SNP-based estimates, where one individual sample that displayed *crypticum*-like morphology sensu Raxworthy & Nussbaum (1996) was grouped with specimens from Mandraka (small body size: APR 12219), while the other two (APR 12201 and APR 12221) clustered with Andasibe specimens and like these were large and of *brevicorne*-like morphology (see Supplementary Table S1 for morphological data). This syntopic occurrence of individuals with divergent phylogenomic histories with distinct morphologies at Anjozorobe may suggest a lack of recent admixture and could thus warrant

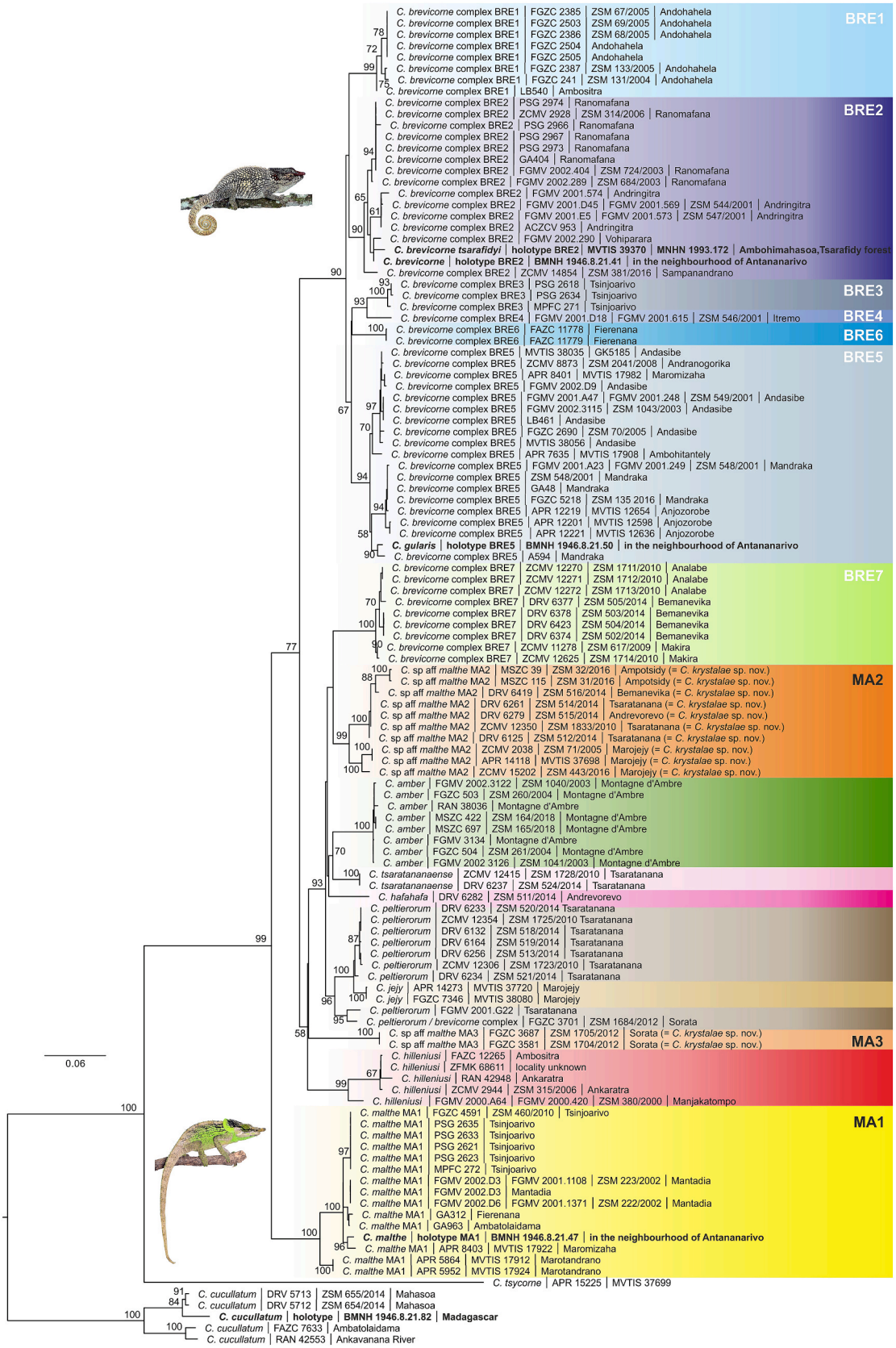

Fig. 4. Maximum Likelihood tree inferred from 2,264 bp of three concatenated mitochondrial DNA fragments (16S, ND2, ND4) in 112 samples of the *Calumma brevicorne* and *C. malthe* clades as defined by the phylogenomic analysis (Fig. 2). Numbers at nodes are bootstrap support values in percent, from an analysis with 500 replicates. *Calumma cucullatum* was used as the outgroup based on the phylogenomic analysis (Fig. 2). Inset photos show representative individuals of the respective clades as in Fig. 3. Type specimens sequenced are in boldface.

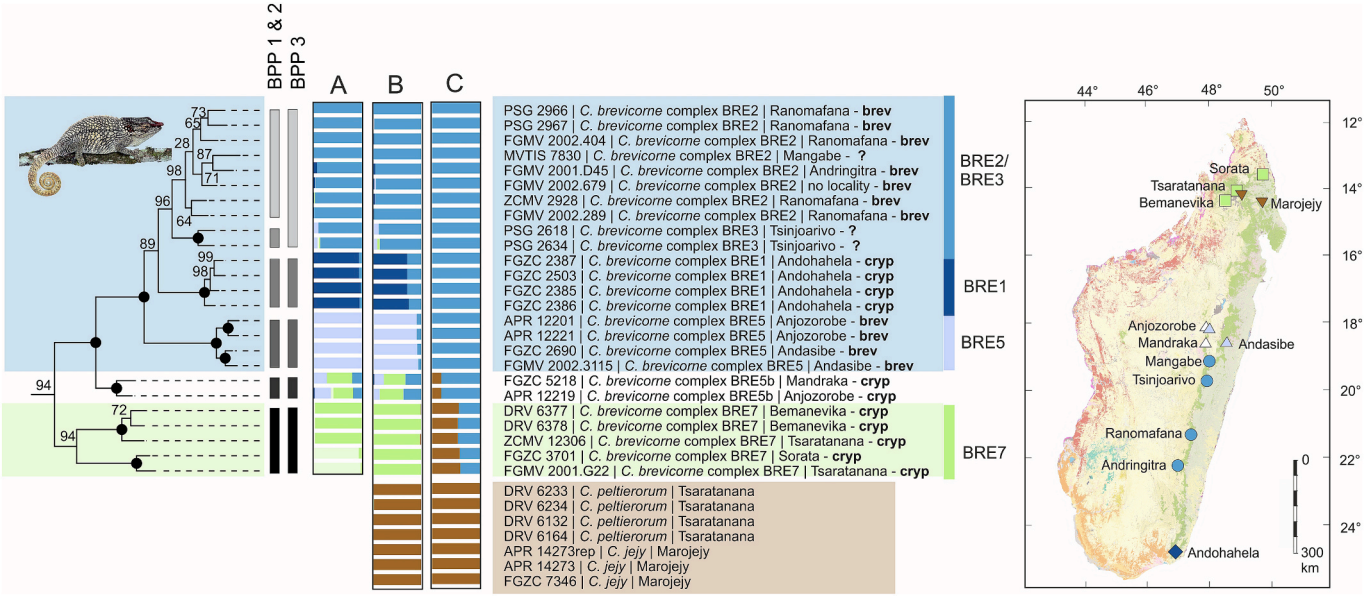

Fig. 5. Assignment of samples and clustering analysis of the *C. brevicorne* complex and *C. peltierorum*. Boldface labels **cryp** and **brev** in tip labels indicate tentative morphological identification of the respective specimens. The tree on the left shows relationships among individuals as in the phylogenomic tree in Fig. 3. Barplots show assignment probabilities to the highest number of genetic clusters retrieved by STRUCTURE for (A) samples of the *C. brevicorne* complex only (K = 5, 5,027 SNPs), (B) samples of *C. brevicorne* complex + *C. peltierorum* (K = 5,211 SNPs), (C) same as B but with K = 2. Analyses with *C. peltierorum* were carried out given indications for mitochondrial introgression with the *C. brevicorne* complex (Fig. 4). Barplots marked with BPP 1 & 2 and BPP 3 indicate the results of a lineage delimitation analysis under the multispecies coalescent, with priors on population size (θ) and divergence time (τ) alternative set to 0.002, (analysis 1), 0.0005 (analysis 2), and 0.02 (analysis 3). Map on the right shows geographical occurrence of the *C. brevicorne* complex samples included in the analysis.

recognition for these lineages as distinct species.

Overall, morphological evidence thus appears to align in part with genetic clustering results. Comparisons are mainly based on males for which we had more material available and which show a more distinct expression of various relevant characters (rostral projection, dorsal and gular crests). Besides the obvious difference in color between specimens from the Andasibe region (stress color of males mostly consisting of beige and whitish color, without blue elements typical for most other populations; Fig. 1), several other differences are apparent between some genetic clusters (data in Table S1): three males of the large form from Andasibe and Anjozorobe (mitochondrial lineage BRE5, but separately clustering based on genomic data; light purple cluster in Fig. 5) attain snout–vent lengths (SVL) of 108–152 mm compared to 67–119 mm in 16 males from other populations. Relative length of the rostral projection (ratio to SVL) was 3.2–4.4 % in BRE5 from Andasibe, 3.1–5.6 % in BRE2, but only 1.3–3.2 % in BRE7.

Based on the Bayesian clustering analysis of the SNP data, up to five or six clusters in the *C. brevicorne* complex could be interpreted as different species (Fig. 5). Also, MSC-based lineage delimitation with BPP (θ and τ priors set to 0.002) supported a model with six subsets (BRE1, BRE2, BRE3, BRE5, BRE5b, BRE7) to be considered as populations or primary species hypotheses (see Sukumaran & Knowles 2017), with a posterior probability of 1.0 (Table S3). The same result was obtained when setting θ and τ priors to 0.0005, while prior settings of 0.02 supported a model with five subsets, merging BRE2 and BRE3 (Table S3). This, along with the syntopic occurrence of morphologically and genetically distinct individuals at Anjozorobe discussed above, suggests the presence of several species in this complex.

However, a taxonomic resolution of the *C. brevicorne* complex is hampered by extensive geographical sampling gaps, and by important nomenclatural hurdles: (i) our analysis lacks RADseq data from Ambohitantely, the type locality of *C. crypticum*; only one mitochondrial sequence from a specimen without type status is available from this site. The name *crypticum* therefore cannot be reliably assigned to one of the genomic clusters identified, given that it is possible that more than one lineage of the complex occurs at this site (as in Anjozorobe). (ii) Large specimens from Andasibe (BRE5) morphologically conform to the current definition of *C. brevicorne* (e.g., Raxworthy & Nussbaum 2006) but according to our museomics results, the oldest available name for the BRE5 genomic cluster is *C. gularis*; while the name *C. brevicorne* would apply to BRE2/BRE3 from the Southern Central East (Andringitra, Ranomafana, Tsinjoarivo, Mangabe). (iii) Introgression/admixture patterns and thus status as evolutionarily independent lineage of specimens from Mandraka and Anjozorobe (BRE5b) and from northern Madagascar (BRE7) are incompletely understood.

3.6. Assessment of species boundaries and taxonomy in the C. malthe clade

Despite mito-nuclear discordance, the systematics of *C. malthe* are less convoluted than in the *C. brevicorne* complex. The genomic data unambiguously reveal two allopatric, deep phylogenomic lineages, one with samples from northern Madagascar and one with samples from the Northern Central East. These lineages are also highly divergent in mtDNA where the northernmost population from Sorata even forms its own lineage. With K = 2, the STRUCTURE analysis neatly identified two unique main populations with little to no signature of admixture (population 1: MA1 l; population 2: MA2 + MA3) (Fig. 6). The maximum number of clusters without ghost lineages was K = 4, with two clusters within MA1 and two within MA2 + MA3, in both cases with indications of admixture over wide geographic gradients of approximately 95 km (from Sorata to Marojejy) and 280 km (from Marotandrano to Maromizaha). MSC-based lineage delimitation with BPP, independent from the prior settings suggested three separate subsets (MA1, MA2, MA3) with posterior probability of 1.0. Also, the haplotype networks for three Sanger-sequenced nuclear-encoded protein-coding gene fragments placed the *C. malthe* clade separate from the *C. brevicorne* clade, and showed no haplotype sharing between samples assigned to MA1 vs. MA2 + MA3 (Supplementary Fig. S4).

Morphological data overall supported these molecular results. Specifically, as detailed in the Diagnosis section below, males of MA2 + MA3 have, in comparison to MA1, a significantly lower number of scales

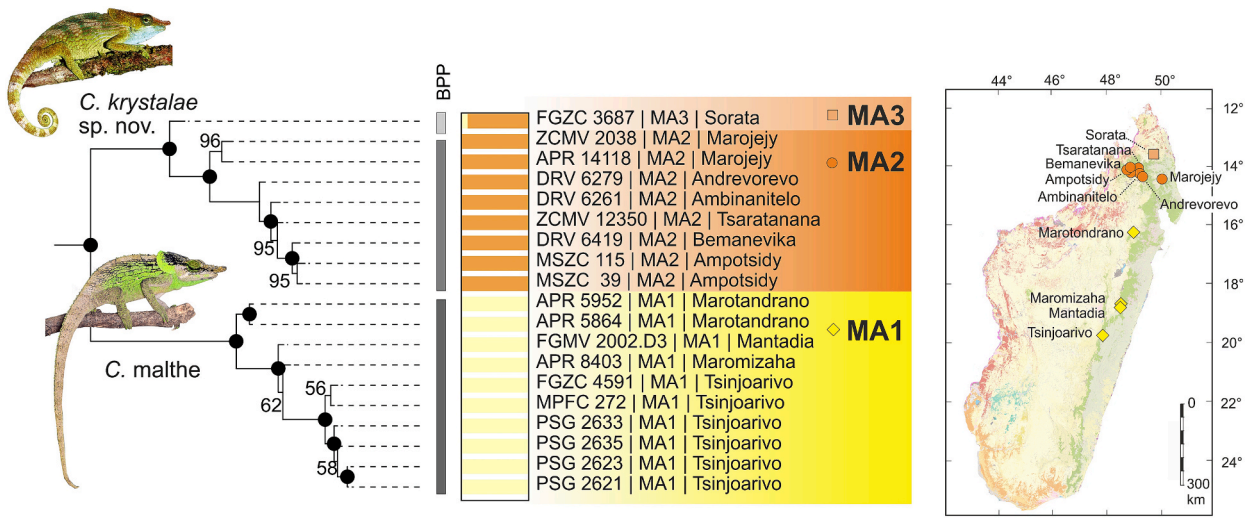

Fig. 6. Assignment of samples of the *C. malthe* clade to clusters inferred by Bayesian clustering analysis with STRUCTURE. The tree on the left shows relationships among individuals as in the phylogenomic tree in Fig. 3. Barplots show assignment results for K = 2 (5,212 SNPs). See Fig. 3 for results of a structure analysis with K = 4. The barplot marked with BPP indicates the results of a lineage delimitation analysis under the multispecies coalescent, with priors on population size (θ) and divergence time (τ) alternative set to 0.002, 0.0005, and 0.02 (all three analysis supported the same partition). Map on the right shows geographical occurrence of the samples included in the analysis.

on the occipital lobes (Table S1), as well as differences in numbers and periodicity of gular and dorsal spines. A more fine-scale comparison between MA2 and MA3 (which BPP resolved as two separate species hypotheses) is hampered by the lack of material (only a single male voucher specimen available for MA3). Based on unambiguous concordance of molecular and morphological data we can however conclude that the northern populations of *C. malthe* represent a distinct species, which we formally describe herein based on specimens of lineage MA2. The Sorata population (MA3) is provisionally assigned to this new species as well but requires future investigation once new material becomes available.

3.7. Conclusions and future directions

Although the supraspecific classification of *Calumma* species was not the primary aim of the present study, the results suggest that profound rearrangements will be necessary to transform the informal phenetic species groups in the genus into more formal, monophyletic groups. This will involve the reallocation of *C. capuroni*, *C. cucullatum* and *C. tsycorne,* clarification of the relationships between the remaining occipital-lobe chameleons with the *C. nasutum* group, which itself might also be paraphyletic (Tolley et al. 2013), and a revision of the enigmatic taxa *C. peyrierasi* and *C. vatosoa*. Our RADseq-derived data have thus revealed the limitations of morphological characters to assign species of chameleons to natural (monophyletic) groups. The large occipital lobes of species such as *C. brevicorne, C. cucullatum,* or *C. malthe* give them a very characteristic appearance and including them together in a species group (Brygoo 1971; Glaw & Vences 1994) seemed an obvious choice, yet our data confirm their non-monophyly (probably polyphyly) already indicated by Tolley et al. (2013).

In the *C. brevicorne* clade, inclusion of additional samples of *C. hafahafa* will allow verification of the status of this morphologically distinctive (Raxworthy & Nussbaum 2006) species for which we here had only a single sample (Fig. 2) and which probably for this reason was not unambiguously identified as separate genetic cluster by STRUCTURE (Fig. 3). The clade also includes various examples of putatively rather young speciation events, such as *C. jejy* and *C. peltierorum* which are morphologically highly divergent (e.g., no rostral projection in male *C. jejy*, different color pattern; Fig. 1) but were not separated into distinct genetic clusters. More in-depth analysis of these two species, with additional samples, especially of the local montane endemic *C. jejy* (only known from high elevations of the Marojejy Massif), could shed more light on the evolutionary processes that promoted recent divergence between these two species. Additionally, a denser geographic sampling from across of the *C. brevicorne* complex is needed to delimit species within the complex and reliably assign the nomina *brevicorne*, *crypticum*, and *gularis*.

Chameleons are highly visual animals and their species-specific phenotypic characters likely play a role in sexual selection (e.g., Parcher 1974; Karsten et al. 2009a, 2009b; Van Kleeck-Hann & Wiens 2023; Glaw et al. 2025). Furthermore, many species also differ conspicuously in genital morphology (Klaver & Böhme 1986), where some differences have also been described between occipital-lobed species such as *C. brevicorne* and *C. malthe* (Brygoo 1971). Examples such as the morphologically distinct sister species *C. jejy* and *C. peltierorum*, connected by rather shallow branches in the molecular trees, illustrate that phenotypic evolution can proceed at a fast pace in chameleons, probably driven at least partly by sexual selection. Under the assumption that sexual isolation might be the strongest barrier to gene flow for sympatric species (Shaw et al. 2024), it could thus be expected that hybridization is rare in chameleons. The multiple instances of mito-nuclear discordance detected by our study, some of which very probably represent ancestral mitochondrial capture, indicate that contrary to these expectations, at least some groups of chameleons may be characterized by complex evolutionary trajectories involving recurrent events of isolation and admixture. Future studies involving whole-genome sequencing, together with detailed quantification of phenotypic characters and sexual dimorphism across populations and species may reveal more in-depth insights into the evolutionary processes underlying phenotypic and genomic evolution as well as species formation of chameleons.

3.8. Taxonomy

The possibility of a separate taxonomic status of specimens from northern Madagascar (Marojejy, Tsaratanana) assigned to *C. malthe* was already considered by Brygoo (1978) who also cited unpublished observations by G. Ramanantsoa in support of this hypothesis. Our new data, with a clear concordance between phylogenomic and morphological evidence, support the status of the northern populations (Fig. 6) as distinct species. As *C. malthe* does not contain any junior synonyms which could be considered as available earlier names for the northern

lineage, in the following we formally name and describe the northern lineage as a new species. A more detailed description, including full details of paratypes and a description of the holotype is found in the supplementary materials.

4. *Calumma krystalae* sp. nov.

LSID: urn:lsid:zoobank.org:act:869550E6-5F33-4704–9520-5B2220BE25E3.

Holotype. ZSM 71/2005 (field number ZCMV 2038), adult male, collected by F. Glaw, M. Vences and R.D. Randrianiaina on 16 February 2005 at Marojejy National Park, Camp 3 "Simpona" (geographical coordinates 14.43665°S, 49.74335°E, 1,326 m a.s.l.), north-eastern Madagascar.

Paratypes. Eleven specimens, comprising eight males and three females: ZSM 1833/2010, 512–516/2014, 443/2016, 1704–1705/2012, 31–32/2016. (for full details, see SI).

Diagnosis. A relatively large *Calumma* assigned to the phenetic *cucullatum* group based on presence of long, bony rostral projection in males, large occipital lobes, and hemipenes with regular calyces extending down much of the truncus and absence of spines. Within the group, adult males can be distinguished from *C. cucullatum, C. jejy* and *C. tsaratananense* by presence of a distinct unpaired rostral projection (vs. absence); from *C. tsaratananense, C. jejy, C. hilleniusi,* and *C. peltierorum* by a poorly developed gular crest with relatively short spines (vs. more strongly developed); from the *C. brevicorne* complex and *C. amber* by occipital lobes separated behind the occiput by only a small notch (vs. large notch); from most species, including *C. peltierorum* and the *C. brevicorne* complex, by a larger number of scales on occipital lobes (at least 160, often > 200, vs. usually < 160) and enlarged scales on

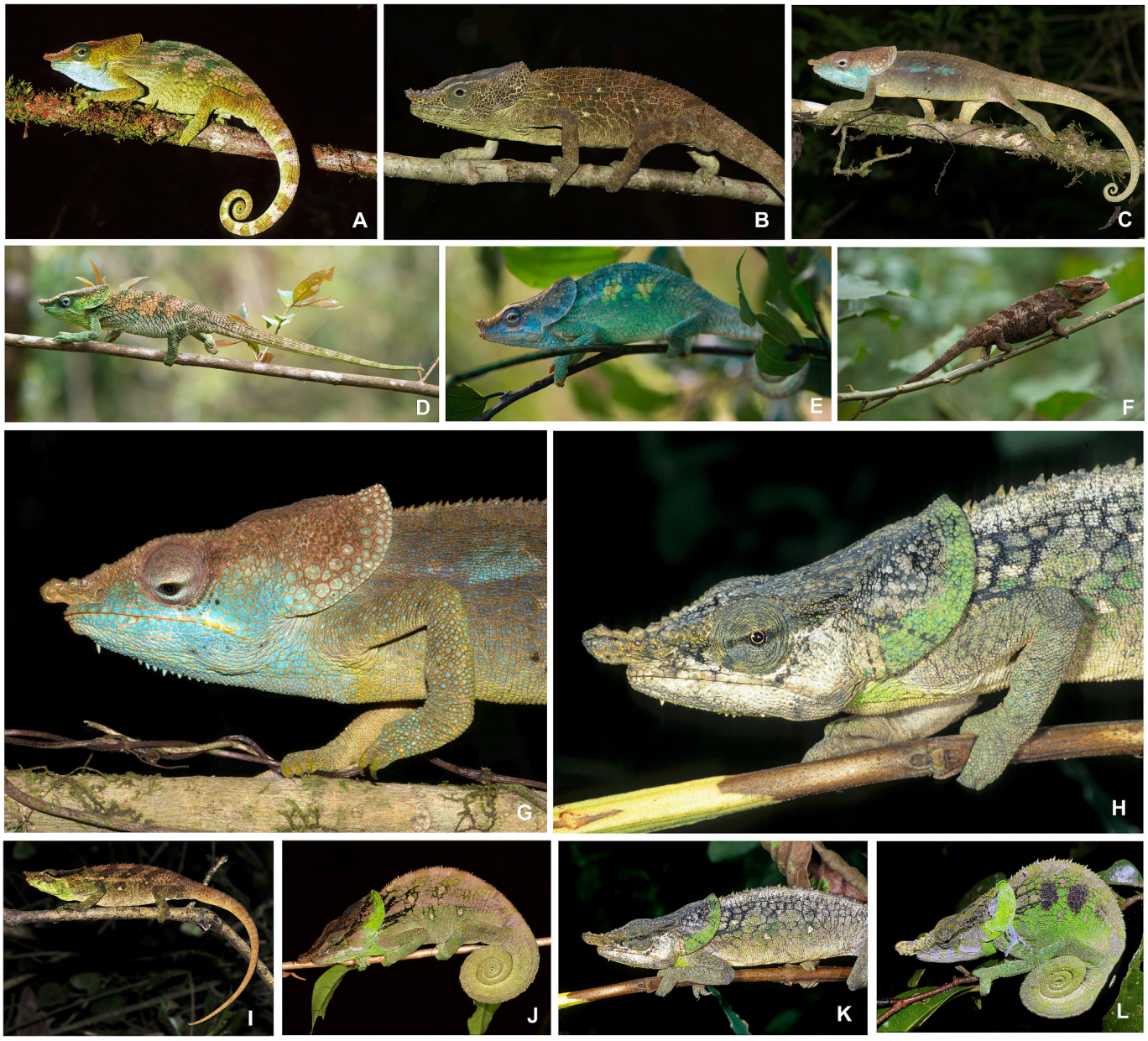

Fig. 7. Photos in life of male specimens of (A–E, G) *Calumma krystalae* sp. nov. and (H–L) *C. malthe*, and (F) one female specimen of *C. krystalae* sp. nov., illustrating the main morphological diagnostic differences between the two species. *C. krystalae* sp. nov.: (A) holotype ZSM 71/2005 from Marojejy; (B) specimen from Marojejy; (C, G) specimen from Sorata; (D) ZCMV 15202 from Marojejy; (E) uncollected male from Ampotsidy; (F) female MSZC 115 from Ampotsidy; *C. malthe*: (H, K, L) precise locality unknown; (I) Tsinjoarivo, (J) Maromizaha. Note uniformly sized spines in dorsal crest in the new species (vs. periodicity in size), and enlarged scales on occipital lobes (vs. scales all of similar size). All photographs by the authors.

occipital lobes smaller (their maximum size usually < 25% of eye diameter vs. usually > 25%). The new species is morphologically most similar to its sister species, *C. malthe*, but differs by a lower number of scales on occipital lobes in most specimens (160–245 vs. 209–441; difference significant in Mann-Whitney *U* test, $P < 0.001$), presence of 6–15 enlarged scales on occipital lobes (their maximum diameter 19–31% of eye diameter, vs. 16–20%), 5–11 spines or spine-like tubercles in gular crest (vs. 1–2); regular arrangement of more or less equally sized dorsal spines (vs. a periodicity with a large spine followed by ca. 5 smaller spines); rostral crest and rostral projection unpigmented, fluorescent under UV light (vs. pigmented with similar color as the remaining surface of head). Based on the limited available data, many of these differences to *C. malthe* also apply to comparisons between females (e.g., size of occipital lobe scales, color of occipital lobes, pigmentation of rostral crest), but may be less obvious.

Description of the holotype. Adult male (Fig. 7A; Fig. S5) with fully everted hemipenes (Fig. S6), in good condition, intact except that a little piece of tongue tissue was removed as tissue sample; SVL 115 mm; tail 153 mm; axilla–groin distance 60.7 mm; horizontal eye diameter 8.5 mm. For full description, see SI. For variation in morphological characters of paratypes, see Table S1 with measurements of scale counts.

Etymology. We dedicate this new species of chameleon to Krystal Tolley, Red List Authority Coordinator for the IUCN Species Survival Commission Chameleon Specialist Group, in recognition of her work on chameleon systematics and conservation. The species epithet is a feminine genitive singular.

Distribution. Taking into account records confirmed by molecular data, the species is known from various high-elevational rainforest sites in northern Madagascar, ranging between 1,280–1,638 m a.s.l.: (1) the type locality Marojejy, (2) the Sorata Massif, (3) the Tsaratanana Massif, (4) Andrevorevo, (5) Bemanevika, (6) Ampotsidy.

Natural History. A rainforest-dwelling species. At Ampotsidy, specimens found at night were roosting on lianas or branches 0.5–2 m above the ground. The species was moderately commonly encountered there, and occurs syntopically with at least four other *Calumma* species (*C. peltierorum*, *C. ratnasariae*, *C. gehringi*, *C. guillaumeti*). Elsewhere, it occurs syntopically with other assemblages of *Calumma*. Most or all specimens observed at Marojejy and Sorata were found at night roosting in the vegetation. In Marojejy (around Camp Simpona), one subadult individual (UADBA-FGZC 7348, not yet studied genetically) was found at night close to a river on 27 March 2025. Other species around this locality were *C. guillaumeti*, *C. uetzi* and juveniles of *C.* cf. *parsonii*.

CRediT authorship contribution statement

Miguel Vences: Writing – original draft, Investigation, Formal analysis, Conceptualization. **Laila-Denise Rothe:** Investigation, Formal analysis. **Frank Glaw:** Writing – review & editing, Resources, Conceptualization. **Mark D. Scherz:** Writing – review & editing, Resources, Conceptualization. **Philip-Sebastian Gehring:** Writing – review & editing, Resources. **Oliver Hawlitschek:** Writing – review & editing, Resources. **Arianna Kuhn:** Writing – review & editing, Resources. **Malte Multzsch:** Writing – review & editing, Investigation. **Alice Petzold:** Writing – review & editing, Investigation. **Michaela Preick:** Writing – review & editing, Investigation. **Fandresena Rakotoarimalala:** Writing – review & editing, Resources. **Achille P. Raselimanana:** Writing – review & editing, Resources. **Fanomezana M. Ratsoavina:** Writing – review & editing, Resources. **Sara Ruane:** Writing – review & editing, Resources. **David R. Vieites:** Writing – review & editing, Resources. **Michael Hofreiter:** Writing – review & editing, Conceptualization. **Christophe Dufresnes:** Writing – review & editing, Investigation, Formal analysis, Conceptualization.

Declaration of competing interest

The authors declare that they have no known competing financial interests or personal relationships that could have appeared to influence the work reported in this paper.

Acknowledgments

This study would not have been possible without the assistance of numerous colleagues, students, and guides during field expeditions in Madagascar; in particular we would like to thank F. Andreone, P. Bora, A. Crottini, F. Mattioli, M. Pabijan, C. Patton, J.L. Patton, E. Rajeriarison, T. Rajoafiarison, R.D. Randriniaina, S. Rasamison, A. Razafimanantsoa, J. Razafindraibe. P. Campbell (London) and N. Vidal (Paris) facilitated examination of historical type material kept under their care. G. Keunecke, Y. Novykova, B. Oetken, and J. Rudolph assisted during laboratory work. Research was carried out in the framework of cooperation accords among the Département de Biologie Animale, Université d'Antananarivo, Madagascar National Parks, the Technische Universität Braunschweig, and the Zoologische Staatssammlung München. Permits for collection and export of specimens were kindly issued by the Ministère de l'Environnement et du Développement Durable of Madagascar. We are grateful to the German Bundesamt für Naturschutz, in particular S. Raths, for kindly issuing numerous CITES import permits over the past decades. This work was supported in part by the Field Museum of Natural History including the Women's Board, the Negaunee Integrative Research Center, the Grainger Bioinformatics Center, the Pritzker Laboratory for Molecular Systematics and Evolution, and the Scholarship Committee, including the African Scholars program; we especially thank Mary and Bruce Feay for their support and S. Goodman for facilitation (Field Museum Negaunee Integrative Research Center, Association Vahatra). The laboratory work was in part supported by the Deutsche Forschungsgemeinschaft (DFG) in the framework of the Taxon-Omics priority program (SPP1991), grant number VE247/19-1, to M. Vences and C. Dufresnes. We are indebted to two anonymous reviewers and to the associate editor for numerous suggestions that helped us to improve earlier versions of the manuscript.

Appendix A. Supplementary data

Supplementary data to this article can be found online at https://doi.org/10.1016/j.ympev.2026.108689. Includes extended description of the new species; Fig. S1, Bayesian clustering analysis for the full dataset; Fig. S2, species tree; Fig. S3, heat map of *f*-branch values; Fig. S4, haplotype networks for three nuclear markers; Fig. S5, photo of preserved holotype of *Calumma krystalae* sp. nov.; Fig. S6, photo of everted hemipenes of *Calumma krystalae* sp. nov.; Table S1 and S2, raw morphometric measurements; Table S3, results of MSC-based lineage delimitation analysis.

Data availability

Raw sequence data are available from the Sequence Read Archive (SRA) under Bioproject PRJNA1462344 (Biosamples SAMN58712888–SAMN58712964). Sanger sequences were submitted to GenBank (accession numbers PZ367831–PZ367833, PZ373022–PZ373357, PZ379204–PZ379207). Assemblies and alignments are available from Zenodo (https://doi.org/10.5281/zenodo.18006710).

References

Andreone, F., Mattioli, F., Jesu, R., Randrianirina, J.E., 2001. Two new chameleons of the genus *Calumma* from north-east Madagascar, with observations on hemipenial morphology in the *Calumma furcifer* group (Reptilia, Squamata, Chamaeleonidae). Herpetol. J. 11, 53–68.

Arévalo, E., Davis, S.K., Sites Jr, J.W., 1994. Mitochondrial DNA-sequence divergence and phylogenetic relationships among eight chromosome races of the *Sceloporus grammicus* complex (Phrynosomatidae) in Central Mexico. Syst. Biol. 43, 387–418.

Avise, J.C., Ball, R.M., 1990. Principles of genealogical concordance in species concepts and biological taxonomy. In: Futuyma, D., Antonovics, J. (Eds.), *Oxford Surveys in Evolutionary Biology*. Oxford University Press, Oxford, pp. 45–67.
Avise, J.C., Wollenberg, K., 1997. Phylogenetics and the origin of species. PNAS 94, 7748–7755.
Böhme, W., 1988. Zur Genitalmorphologie der Sauria: Funktionelle und stammesgeschichtliche Aspekte. Bonner Zool. Monogr. 27, 1–165.
Bonnet, T., Leblois, R., Rousset, F., Crochet, P.A., 2017. A reassessment of explanations for discordant introgressions of mitochondrial and nuclear genomes. Evolution 71, 2140–2158.
Bouckaert, R.R., 2010. DensiTree: making sense of sets of phylogenetic trees. Bioinformatics 26, 1372–1373.
Bouckaert, R., Vaughan, T.G., Barido-Sottani, J., Duchêne, S., Fourment, M., Gavryushkina, A., Heled, J., Jones, G., Kühnert, D., De Maio, N., Matschiner, M., Mendes, F.K., Müller, N.F., Ogilvie, H.A., du Plessis, L., Popinga, A., Rambaut, A., Rasmussen, D., Siveroni, I., Suchard, M.A., Wu, C.H., Xie, D., Zhang, C., Stadler, T., Drummond, A.J., 2019. BEAST 2.5: an advanced software platform for Bayesian evolutionary analysis. PLoS Comput. Biol. 15, e1006650.
Boumans, L., Vieites, D.R., Glaw, F., Vences, M., 2007. Geographical patterns of deep mitochondrial differentiation in widespread Malagasy reptiles. Mol. Phylogenet. Evol. 45, 822–839.
Brelsford, A., Dufresnes, C., Perrin, N., 2016. High-density sex-specific linkage maps of a European tree frog (*Hyla arborea*) identify the sex chromosome without information on offspring sex. Heredity 116, 177–181.
Brygoo, E.R., 1971. Reptiles Sauriens Chamaeleonidae - Genre *Chamaeleo*. Faune De Madagascar 33, 1–318.
Brygoo, E.R., 1978. Reptiles Sauriens Chamaeleonidae. Genre *Brookesia* et complément pour le genre *Chamaeleo*. *Faune de Madagascar* 47, 1–173.
Brygoo, E.R., Domergue, C.A., 1967. Description d'un Caméléon nouveau de Madagascar *Chamaeleo tsaratananensis* n. sp. Bull. Mus. Natl. Hist. Nat Paris 39, 829–832.
Brygoo, E.R., Domergue, C.A., 1970. Notes sur les *Chamaeleo* de Madagascar. *C. brevicornis* Gunther, 1879, *tsarafidyi* nov. subsp. Les hémipénis des Caméléons du groupe *brevicornis*. Bull. Mus. Natl. Hist. Nat Paris 42, 311–320.
Brygoo, E.R., Blanc, C.P., Domergue, C.A., 1972. Notes sur les *Chamaeleo* de Madagascar. X. Deux nouveaux Caméléons des hauts sommets de Madagascar: *C. capuroni* n.sp. et *C. gastrotaenia andringitraensis* n.subsp. Bull. Mus. Natl. Hist. Nat. Paris 42, 601–613.
Brygoo, E.R., Blanc, C.P., Domergue, C.A., 1973. Notes sur les *Chamaeleo* de Madagascar. XI. Un nouveau Caméléon de l'Ankaratra: *C. brevicornis hilleniusi* n.subsp. Bull. Soc. Zool. France 98, 113–120.
Camacho, C., Coulouris, G., Avagyan, V., Ma, N., Papadopoulos, J., Bealer, K., Madden, T.L., 2009. BLAST+: architecture and applications. BMC Bioinf. 10, 421.
Campbell, P.D., Denzer, W., 2019. Annotated catalogue of chameleon types in the collection of the Natural History Museum, UK (NHMUK) (Reptilia: Squamata: Chamaeleonidae). Zootaxa 4742, 481–500.
Catchen, J., Hohenlohe, P.A., Bassham, S., Amores, A., Cresko, W.A., 2013. Stacks: an analysis tool set for population genomics. Mol. Ecol. 22, 3124–3140.
Conroy, C.J., Papenfuss, T., Parker, J., Hahn, N., 2009. Use of tricaine methanesulfonate (MS-222) for euthanasia of reptiles. J. Am. Assoc. Lab. Anim. Sci. 48, 28–32.
Dabney, J., Knapp, M., Glocke, I., Gansauge, M.-T., Weihmann, A., Nickel, B., Valdiosera, C., García, N., Pääbo, S., Arsuaga, J.-L., Meyer, M., 2013. Complete mitochondrial genome sequence of a Middle Pleistocene cave bear reconstructed from ultrashort DNA fragments. PNAS 110, 15758–15763.
de Queiroz, K., 1998. The General Lineage Concept of species, species criteria, and the process of speciation. In: Howard, D.J., Berlocher, S.H. (Eds.), *Endless Forms: Species and Speciation*. Oxford University Press, Oxford, pp. 57–75.
de Queiroz, K., 2007. Species concepts and species delimitation. Syst. Biol. 56, 879–886.
Dollion, A.Y., Herrel, A., Marquis, O., Leroux-Coyau, M., Meylan, S., 2020. The colour of success: does female mate choice rely on male change in the chameleon *Furcifer pardalis*? J. Exp. Biol. 223 (Pt 20), jeb224550.
Dufresnes, C., Brelsford, A., Jeffries, D.L., Mazepa, G., Suchan, T., Canestrelli, D., Nicieza, A., Fumagalli, L., Dubey, S., Martínez-Solano, I., Litvinchuk, S.N., Vences, M., Perrin, N., Crochet, P.A., 2021. Mass of genes rather than master genes underlie the genomic architecture of amphibian speciation. PNAS 118, e2103963118.
Dufresnes, C., Poyarkov, N., Jablonski, D., 2023. Acknowledging more biodiversity without more species. PNAS 120, e2302424120.
Dufresnes, C., Jablonski, D., Ambu, J., Prasad, V., Bala Gautam, K., Kamei, R.G., Mahony, S., Hofmann, S., Masroor, R., Alard, B., Crottini, A., Edmonds, D., Ohler, A., Jiang, J., Khatiwada, J., Gupta, S.K., Borzée, A., Borkin, L., Skorinov, D., Melnikov, D.A., Milto, K., Konstantinov, E.L., Künzel, S., Suchan, T., Arkhipov, D., Trofimets, A., Nguyen, T.V., Suwannapoom, C., Litvinchuk, S.N., Poyarkov, N.A., 2025. Speciation and historical invasions of the asian black-spined toad (*Duttaphrynus melanostictus*). Nat. Commun. 16, 298.
Falush, D., Stephens, M., Pritchard, J.K., 2003. Inference of population structure using multilocus genotype data: linked loci and correlated allele frequencies. Genetics 164, 1567–1587.
Flouri, T., Jiao, X., Rannala, B., Yang, Z., 2018. Species tree inference with BPP using genomic sequences and the multispecies coalescent. Mol. Biol. Evol. 35, 2585–2593.
Fong, J.J., Blom, M.P., Aowphol, A., McGuire, J.A., Sutcharit, C., Soltis, P.S., 2023. Recent advances in museomics: revolutionizing biodiversity research. Front. Ecol. Evol. 11, 1188172.
Fulton, T.L., Shapiro, B., 2019. Setting up an ancient DNA laboratory. In: Shapiro, B., Barlow, A., Heintzman, P.D., Hofreiter, M., Paijmans, J.L.A., Soares, A.E.R. (Eds.), *Ancient DNA: Methods and Protocols*. Springer, New York, pp. 1–13.
Gansauge, M.-T., Gerber, T., Glocke, I., Korlević, P., Lippik, L., Nagel, S., Riehl, L.M., Schmidt, A., Meyer, M., 2017. Single-stranded DNA library preparation from highly degraded DNA using T4 DNA ligase. Nucleic Acids Res. 45, e79.
Gehring, P.-S., Pabijan, M., Ratsoavina, F.M., Köhler, J., Vences, M., Glaw, F., 2010. A Tarzan yell for conservation: a new chameleon, *Calumma tarzan* sp. n., proposed as a flagship species for the creation of new nature reserves in Madagascar. Salamandra 46, 167–179.
Gehring, P.-S., Tolley, K.A., Eckhardt, F.S., Townsend, T.M., Ziegler, T., Ratsoavina, F., Glaw, F., Vences, M., 2012. Hiding deep in the trees: discovery of divergent mitochondrial lineages in Malagasy chameleons of the *Calumma nasutum* group. Ecol. Evol. 2, 1468–1479.
Gippner, S., Strowbridge, N., Šunje, E., Capstick, M., Amat, F., Bogaerts, S., Merabet, K., Preissler, K., Galán, P., Martínez-Solano, I., Bonato, L., Steinfartz, S., Velo-Antón, G., Dufresnes, C., Elmer, K.R., Vences, M., 2024. The effect of hybrids on phylogenomics and subspecies delimitation in *Salamandra*, a highly diversified amphibian genus. Salamandra 60, 105–128.
Glaw, F., 2015. Taxonomic checklist of chameleons (Squamata: Chamaeleonidae). Vertebr. Zool. 65, 167–246.
Glaw, F., Vences, M., 1992. *A Fieldguide to the Amphibians and Reptiles of Madagascar*. Vences & Glaw, Köln, p. 331.
Glaw, F., Vences, M., 1994. *A Fieldguide to the Amphibians and Reptiles of Madagascar*, 2nd Edition, including Mammals and Freshwater Fish. Vences & Glaw, Köln, 480 pp.
Glaw, F., Vences, M., 2007. *A Field Guide to the Amphibians and Reptiles of Madagascar*, 3rd Edition. Vences & Glaw Verlag, 496 pp.
Glaw, F., Köhler, J., Townsend, T.M., Vences, M., 2012. Rivaling the world's smallest reptiles: discovery of miniaturized and microendemic new species of leaf chameleons (*Brookesia*) from northern Madagascar. PLoS One 7, e31314.
Glaw, F., Hawlitschek, O., Ruthensteiner, B., 2013. A new genus name for an ancient Malagasy chameleon clade and a PDF-embedded 3D model of its skeleton. Salamandra 49, 237–238.
Glaw, F., Agne, S., Prötzel, D., Gehring, P.-S., Köhler, J., Preick, M., Ratsoavina, F.M., Straube, N., Wollenberg Valero, K., Crottini, A., Vences, M., 2025. Towards a revision of the Malagasy chameleons of the *Calumma gallus* complex: Redefinition of *Calumma nasutum* based on a museomics approach and descriptions of two new species. Salamandra 61, 442–466.
Gray, J.E., 1831. A synopsis of the species of Class Reptilia. In: Griffith, E., Pidgeon, E. *The Animal Kingdom arranged in conformity with its organisation by the Baron Cuvier, with additional descriptions of all the species hitherto named, and of many not before noticed*. Whittaker, Treacher and Co., London, pp. 481 + 110.
Grbic, D., Saenko, S.V., Randriamoria, T.M., Debry, A., Raselimanana, A.P., Milinkovitch, M.C., 2015. Phylogeography and support vector machine classification of colour variation in panther chameleons. Mol. Ecol. 24, 3455–3466.
Günther, A., 1879. Description of four new species of *Chamaeleon* from Madagascar. Proc. Zool. Soc. Lond. 1879, 148–150.
Han, D., Zhou, K., Bauer, A.M., 2004. Phylogenetic relationships among gekkotan lizards inferred from C-mos nuclear DNA sequences and a new classification of the Gekkota. Biol. J. Linn. Soc. 83, 353–368.
Hoang, D.T., Chernomor, O., Von Haeseler, A., Minh, B.Q., Vinh, L.S., 2018. UFBoot2: improving the ultrafast bootstrap approximation. Mol. Biol. Evol. 35, 518–522.
Kalyaanamoorthy, S., Minh, B.Q., Wong, T.K., Von Haeseler, A., Jermiin, L.S., 2017. ModelFinder: fast model selection for accurate phylogenetic estimates. Nat. Methods 14, 587–589.
Karin, B.R., Frederick, J.H., Hamidy, A., Riyanto, A., Arida, E., Iskandar, D.T., Das, I., Shabrani, A., Quah, E.S.H., Jackman, T.R., Bauer, A.M., McGuire, J.A., 2025. When islands collide: divergence predicts outcomes of secondary contact during the fusion of Sulawesi's paleo-archipelago. PNAS 122, e2514344122.
Karsten, K.B., Andriamandimbiarisoa, L.N., Fox, S.F., Raxworthy, C.J., 2009a. Behavior of two species of chameleons in Madagascar: Insights into sexual selection. Herpetologica 65, 54–69.
Karsten, K.B., Andriamandimbiarisoa, L.N., Fox, S.F., Raxworthy, C.J., 2009b. Sexual selection on body size and secondary sexual characters in 2 closely related, sympatric chameleons in Madagascar. Behav. Ecol. 20, 1079–1088.
Katoh, K., Standley, D.M., 2013. MAFFT multiple sequence alignment software version 7: Improvements in performance and usability. Mol. Biol. Evol. 30, 772–780.
Keren-Rotem, T., Main, D.C., Barocas, A., Donaire-Barroso, D., Haddas-Sasson, M., Vila, C., Shaharabany, T., Wolf, L., Tolley, K.A., Geffen, E., 2024. Genetic and behavioural factors affecting interpopulation colour pattern variation in two congeneric chameleon species. R. Soc. Open Sci. 11, 231554.
Klaver, C., Böhme, W., 1986. Phylogeny and classification of the Chamaeleonidae (Sauria), with special reference to hemipenis morphology. Bonn. Zool. Monogr. 22, 1–64.
Klaver, C., Böhme, W., 1997. Chamaeleonidae. Das Tierreich 112, 1–85.
Kumar, S., Stecher, G., Tamura, K., 2016. MEGA7: molecular evolutionary genetics analysis version 7.0 for bigger datasets. Mol. Biol. Evol. 33, 1870–1874.
Macey, J.R., Larson, A., Ananjeva, N.B., Fang, Z., Papenfuss, T.J., 1997. Two novel gene orders and the role of light-strand replication in rearrangement of the vertebrate mitochondrial genome. Mol. Biol. Evol. 14, 91–104.
Macey, J.R., Schulte, J.A., Larson, A., Fang, Z., Wang, Y., Tuniyev, B.S., Papenfuss, T.J., 2000. Evaluating trans-Tethys migration: an example using acrodont lizard phylogenetics. Syst. Biol. 49, 233–256.
Malinsky, M., Matschiner, M., Svardal, H., 2021. Dsuite—Fast D-statistics and related admixture evidence from VCF files. Mol. Ecol. Resour. 21, 584–595.
Martin, M., 2011. Cutadapt removes adapter sequences from high-throughput sequencing reads. Embnet.journal 17, 10–12.
Matschiner, M., 2016. Fitchi: haplotype genealogy graphs based on the Fitch algorithm. Bioinformatics 32, 1250–1252.

Minh, B.Q., Schmidt, H.A., Chernomor, O., Schrempf, D., Woodhams, M.D., von Haeseler, A., Lanfear, R., 2020. IQ-TREE 2: new models and efficient methods for phylogenetic inference in the genomic era. Mol. Biol. Evol. 37, 1530–1534.
Nielsen, S.V., Banks, J.L., Diaz Jr., R.E., Trainor, P.A., Gamble, T., 2018. Dynamic sex chromosomes in Old World chameleons (Squamata: Chamaeleonidae). J. Evol. Biol. 31, 484–490.
Padial, J.M., Miralles, A., De la Riva, I., Vences, M., 2010. The integrative future of taxonomy. Front. Zool. 7, 16.
Paijmans, J.L.A., Baleka, S., Henneberger, K., Taron, U.H., Trinks, A., Westbury, M.V., Barlow, A., 2017. Sequencing single-stranded libraries on the Illumina NextSeq 500 platform. *arXiv* 1711.11004.
Pang, X.-X., Zhang, D.-Y., 2025. A cautionary note on using STRUCTURE to detect hybridization in a phylogenetic context. J. Syst. Evol. 63, 843–858.
Parcher, S.R., 1974. Observations on the natural histories of six Malagasy Chamaeleontidae. Z. Tierpsychol. 34, 500–523.
Paris, J.R., Stevens, J.R., Catchen, J.M., 2017. Lost in parameter space: a road map for stacks. Methods Ecol. Evol. 8, 1360–1373.
Pritchard, J.K., Stephens, M., Donnelly, P., 2000. Inference of population structure using multilocus genotype data. Genetics 155, 945–959.
Prötzel, D., Ruthensteiner, B., Glaw, F., 2016. No longer single! Description of female *Calumma vatosoa* (Squamata, Chamaeleonidae) including a review of the species and its systematic position. Zoosyst. Evol. 92, 13–21.
Prötzel, D., Lambert, S.M., Andrianasolo, G.T., Hutter, C.R., Cobb, K.A., Scherz, M.D., Glaw, F., 2018a. The smallest 'true chameleon' from Madagascar: a new, distinctly colored species of the *Calumma boettgeri* complex (Squamata, Chamaeleonidae). Zoosyst. Evol. 94, 409–423.
Prötzel, D., Vences, M., Hawlitschek, O., Scherz, M.D., Ratsoavina, F.M., Glaw, F., 2018b. Endangered beauties: micro-CT cranial osteology, molecular genetics and external morphology reveal three new species of chameleons in the *Calumma boettgeri* complex (Squamata: Chamaeleonidae). Zool. J. Linn. Soc. 184, 471–498.
Prötzel, D., Scherz, M.D., Ratsoavina, F.M., Vences, M., Glaw, F., 2020. Untangling the trees: revision of the *Calumma nasutum* complex (Squamata: Chamaeleonidae). Vertebr. Zool. 70, 23–59.
Puillandre, N., Brouillet, S., Achaz, G., 2021. ASAP: assemble species by automatic partitioning. Mol. Ecol. Resour. 21, 609–620.
Rambaut, A., Drummond, A.J., Xie, D., Baele, G., Suchard, M.A., 2018. Posterior summarization in Bayesian Phylogenetics using Tracer 1.7. Syst. Biol. 67, 901–904.
Raxworthy, C.J., Nussbaum, R.A., 2006. Six new species of occipital-lobed *Calumma* chameleons (Squamata: Chamaeleonidae) from montane regions of Madagascar, with a new description and revision of *Calumma brevicorne*. Copeia 2006, 711–734.
Raxworthy, C.J., Forstner, M.R.J., Nussbaum, R.A., 2002. Chameleon radiation by oceanic dispersal. Nature 415, 784.
Rochette, N.C., Rivera-Colón, A.G., Catchen, J.M., 2019. Stacks 2: Analytical methods for paired-end sequencing improve RADseq-based population genomics. Mol. Ecol. 28, 4737–4754.
Rohland, N., Siedel, H., Hofreiter, M., 2004. Nondestructive DNA extraction method for mitochondrial DNA analyses of museum specimens. Biotechniques 36, 814–821.
Salzburger, W., Ewing, G.B., von Haeseler, A., 2011. The performance of phylogenetic algorithms in estimating haplotype genealogies with migration. Mol. Ecol. 20, 1952–1963.
Shaw, K.L., Cooney, C.R., Mendelson, T.C., Ritchie, M.G., Roberts, N.S., Yusuf, L.H., 2024. How important is sexual isolation to speciation? Cold Spring Harb. Perspect. Biol. 16, a041427.
Shen, X.-X., Liang, D., Zhang, P., 2012. The development of three long universal nuclear protein-coding locus markers and their application to osteichthyan phylogenetics with nested PCR. PLoS One 7, e39256.
Shylo, N.A., Price, A.J., Robb, S., Kupronis, R., Méndez, I.A.G., DeGraffenreid, D., Gamble, T., Trainor, P.A., 2024. *Chamaeleo calyptratus* (veiled chameleon) chromosome-scale genome assembly and annotation provides insights into the evolution of reptiles and developmental mechanisms. bioRxiv. https://doi.org/10.1101/2024.09.03.611012.
Speybroeck, J., Beukema, W., Dufresnes, C., Fritz, U., Jablonski, D., Lymberakis, P., Martínez-Solano, I., Razzetti, E., Vamberger, M., Vences, M., Vörös, J., Crochet, P.A., 2020. Species list of the European herpetofauna – 2020 update by the taxonomic committee of the Societas Europaea Herpetologica. Amphibia-Reptilia 41, 139–189.
Steenwyk, J.L., Li, Y., Zhou, X., Shen, X.X., Rokas, A., 2023. Incongruence in the phylogenomics era. Nat. Rev. Genet. 24, 834–850.
Stephens, M., Smith, N.J., Donnelly, P., 2001. A new statistical method for haplotype reconstruction from population data. Am. J. Hum. Genet. 68, 978–989.
Stoltz, M., Baeumer, B., Bouckaert, R., Fox, C., Hiscott, G., Bryant, D., 2021. Bayesian inference of species trees using diffusion models. Syst. Biol. 70, 145–161.
Straube, N., Lyra, M.L., Paijmans, J.L.A., Preick, M., Basler, N., Penner, J., Rödel, M.-O., Westbury, M.V., Haddad, C.F., Barlow, A., Hofreiter, M., 2021. Successful application of ancient DNA extraction and library construction protocols to museum wet collection specimens. Mol. Ecol. Resour. 21, 2299–2315.
Stuart-Fox, D., Moussalli, A., 2008. Selection for social signalling drives the evolution of chameleon colour change. PLoS Biol. 6, e25.
Sukumaran, J., Knowles, L.L., 2017. Multispecies coalescent delimits structure, not species. PNAS 114, 1607–1612.
Taft, J.M., Tolley, K.A., Alexander, G.J., Geneva, A.J., 2023. De novo whole genome assemblies for two Southern African dwarf chameleons (Bradypodion, Chamaeleonidae). Genome Biol. Evol. 15, evad182.
Teyssier, J., Saenko, S.V., Van Der Marel, D., Milinkovitch, M.C., 2015. Photonic crystals cause active colour change in chameleons. Nature Comm. 6, 6368.
Toews, D.P., Brelsford, A., 2012. The biogeography of mitochondrial and nuclear discordance in animals. Mol. Ecol. 21, 3907–3930.
Tolley, K.A., Herrel, A. (Eds.), 2013. *The Biology of Chameleons*. University of California Press, Berkeley, p. 275.
Tolley, K.A., Townsend, T.M., Vences, M., 2013. Large-scale phylogeny of chameleons suggests african origins and Eocene diversification. Proc. R. Soc. B 280, 20130184.
Uetz, P., Freed, P., Aguilar, R., Reyes, F., Kudera, J., Hošek, J. (Eds.), 2026. The Reptile Database. http://www.reptile-database.org (accessed 18 May 2026).
Van Kleeck-Hann, M., Wiens, J.J., 2023. Macroevolution of sexually selected weapons: weapon evolution in chameleons. Evolution 77, 2277–2290.
Vences, M., Miralles, A., Brouillet, S., Ducasse, J., Fedosov, A., Kharchev, V., Kostadinov, I., Kumari, S., Patmanidis, S., Scherz, M.D., Puillandre, N., Renner, S.S., 2021. iTaxoTools 0.1: Kickstarting a specimen-based software toolkit for taxonomists. Megataxa 6, 77–92.
Vences, M., Patmanidis, S., Kharchev, V., Renner, S.S., 2022. Concatenator, a user-friendly program to concatenate DNA sequences, implementing graphical user interfaces for MAFFT and FastTree. Bioinform. Adv. 2, vbac050.
Vences, M., Patmanidis, S., Schmidt, J.-C., Matschiner, M., Miralles, A., Renner, S.S., 2024. Hapsolutely: a user-friendly tool integrating haplotype phasing, network construction and haploweb calculation. Bioinform. Adv. 4, vbae083.
Vences, M., Patmanidis, S., Kulikov, N., Irisarri, I., Schulz, A.-K., Rothe, L.-D., Petzold, A., Scherz, M.D., 2026. BlasTax—a user-friendly stand-alone tool to leverage the BLAST + program for molecular taxonomy. Megataxa 19, 457–468.
Whiting, M.J., Holland, B.S., Keogh, J.S., Noble, D.W.A., Rankin, K.J., Stuart-Fox, D., 2022. Invasive chameleons released from predation display more conspicuous colors. Sci. Adv. 8, eabn2415.
Xie, H., Chen, Z., Pang, S., Du, W., 2023. Efficient and highly continuous chromosome-level genome assembly of the first chameleon genome. Genome Biology and Evolution 15, evad131.